NACA RM L50D07

NACA

RESEARCH MEMORANDUM

PRESSURE-RISE AND LEAKAGE-LOSS CHARACTERISTICS OF A ROTATING COWLING

By Jack F. Runckel and Gerald Hieser

Langley Aeronautical Laboratory
Langley Air Force Base, Va.

NATIONAL ADVISORY COMMITTEE
FOR AERONAUTICS
WASHINGTON

August 30, 1950
Declassified December 11, 1953

NACA RM L50D07

NATIONAL ADVISORY COMMITTEE FOR AERONAUTICS

RESEARCH MEMORANDUM

PRESSURE-RISE AND LEAKAGE-LOSS CHARACTERISTICS OF A ROTATING COWLING

By Jack F. Runckel and Gerald Hieser

SUMMARY

An experimental and analytical investigation was conducted for the purpose of studying the pressure-rise and leakage-loss characteristics of rotating cowlings. The internal-flow characteristics of the test cowling were investigated over a broad range of the flow parameters and a method for determining the pressure-rise characteristics has been derived.

A comparison of the experimental and analytical results indicates that the pressure-rise characteristics can be predicted if the internal-flow losses and the internal-flow angle at the cowling-vane trailing edge are known.

The total-pressure losses through the leak gap were of negligible magnitude for all conditions investigated. The flow lost through the leak gap varied from about 5 percent to more than 25 percent of the inlet flow. The leak flow was greatest at low inlet-velocity ratios and at high values of vane pressure rise.

Some of the features peculiar to the design of rotating cowlings are discussed and methods for estimating the leak flow and the proper setting of the cowling vane are included.

INTRODUCTION

The use of a rotating cowling for propeller-driven aircraft has been advocated from time to time. This type of cowling, sometimes referred to as an E-type cowling, consists of inner and outer rotating shells held together by streamline fairings which cover the propeller blade shanks. The internal air flow is inducted through the spaces enclosed by the shells and fairings. The blade-shank fairings or vanes, which are in the form of airfoil sections, are fixed within the rotating

cowling, and operate at an effective angle of attack determined by the ratio of internal volume flow to the cowling rotational speed.

Little information on the internal aerodynamics of rotating cowlings has been published. Some previous investigations have been conducted to study the drag characteristics (references 1 and 2). Flight and ground-cooling tests of an air-cooled engine equipped with a rotating cowling are reported in reference 3. Wind-tunnel-model tests of a rotating cowling to determine the effect of the spinner-body gap on the pressures available for cooling are presented in reference 4. More recently the British have conducted model tests to investigate the drag, power requirements, and cooling characteristics of hollow spinner fans (reference 5). Whirl tests of a rotating cowling are reported in references 6 and 7.

The purpose of the present investigation is to study experimentally and analytically the pressure-rise and leakage-loss characteristics of a rotating cowling. The cowling used in the experimental phase of the investigation was an adaptation of the one described in reference 7 altered to fit a nacelle available in the Langley 16-foot high-speed tunnel. The cowling aerodynamic investigation was one phase of a comprehensive engine-cowling study, the other phases of which were subsequently cancelled. The pressure-rise and leakage-flow characteristics were investigated over a broad range of internal-flow parameters. The pressure rise of the cowling was also calculated analytically. Although the configuration tested incorporated some features which limited the efficiency of the cowling, the experimental results provide a check on the manner in which the pressure rise varies with the internal-flow parameters.

The design of rotating cowlings is discussed on the basis of the internal-flow analysis and the observed experimental trends. Methods for estimating the leakage losses and the proper vane setting are outlined.

SYMBOLS

H	total pressure, pounds per square foot
ΔH	total pressure difference, pounds per square foot
p	static pressure, pounds per square foot
q	dynamic pressure, pounds per square foot
ρ	mass density of air, slugs per cubic foot
N	cowling rotational speed, revolutions per minute

n	cowling rotational speed, revolutions per second
U	vane section rotational velocity, feet per second $(2\pi rn)$
ω	angular velocity of vane, radians per second
u	rotational velocity of air, feet per second
V	velocity, feet per second
W	resultant velocity of air relative to vane, feet per second
Q	quantity flow, cubic feet per second
A	cross-sectional area, square feet
d	root-mean-square diameter, feet
R	radius to outer wall of annulus, feet
r	radius, feet
C	orifice coefficient
k	pressure-loss coefficient
θ	angle between axial velocity vector and resultant velocity vector of air at trailing edge of vane, degrees
ψ	angle between axial direction and velocity vector leaving leak gap, degrees

Subscripts: The numerical subscripts refer to stations shown in figure 1.

1	cowling inlet
2	leading edge of vane
3	trailing edge of vane
4	exit of leak gap
5	survey station behind vane
a	axial component
L	leak

l	local
o	free stream
r	resultant
LE	leading edge of vane
s	surface
calc	calculated

MODEL CONFIGURATION

The present rotating cowling was built from a "blower spinner," described in reference 7, originally constructed by the Hamilton Standard Propeller Company for an installation utilizing a Wright R-2600 engine and was altered for these tests to fit an available nacelle utilizing a Pratt & Whitney R-2800-31 engine. A sketch of the model installation tested is shown as figure 1. The rotating cowling as constructed retained the original Hamilton Standard propeller and hub, the original mounting attachments, and the original outer shell; but the annular passage was redesigned to fit the Pratt & Whitney engine.

Preliminary tests showed that severe separation occurred from the inner surface of the cowling lip. A modification of the leading edge to alleviate this condition was incorporated in the form of a balsa filler attached to the lip as shown in figure 2. A plot of flow area through the cowling with the filler installed is also shown in figure 2.

The rotating cowling was made up of two sections, the front section which was detachable to permit removal of the propeller dome, and the rear section which contained the propeller shanks. Photographs of the front section, the rear section, and the assembled cowling are shown in figures 3, 4, and 5, respectively. All circular shells and structural members were fabricated from aluminum spinnings. The vanes were made of heat-treated sheet duralumin and were riveted to the spinnings forming the air passage. The total testing time, including the time for whirl, preliminary, and performance tests, was approximately 160 hours. Upon completion of the investigation no sign of fatigue failure could be detected.

A concept of rotating cowling design is that the vanes should provide zero or small pressure rise at the high-speed condition because additional pressure rise is not required for this condition and minimum cowling input power is desired. If this concept is followed, the vanes

should be constructed in the shape of airfoil sections warped to fit the air helix path at the design condition. For the present cowling it was intended that the vane root, mean, and tip radius sections be alined with the respective helix paths. However, because of errors in the design, alterations to facilitate construction, and the addition of the balsa filler, the vanes were not alined completely with any mean air path based on the internal geometry and given values of Q_1 and n. The vanes utilized an altered 16-series thickness distribution and were about 25 percent thick at the mean radius section to permit full feathering operation of the propeller. The vane sides were generated by straight-line elements extending from the axis of rotation to the surface of the airfoil section located at the mean radius of the annular passage. A representation of the vane shape at the root-mean-square radius of the annular passage is shown in the sketch of figure 6. The forward portion (shown as dotted lines) is distorted considerably as a result of the rapidly changing radius, but the distortion is negligible near the trailing edge. Included on the figure are the mean line of the vane section and the air helix path which most nearly corresponds to the mean line along the rear portion of the vane. The forward portions of the vane are effectively at local angles of attack with respect to the curved flow of the illustrated air helix. This local angle is accentuated by the addition of the balsa filler.

A fixed diffuser which directed air to the engine cyclinders was located directly behind the trailing edge of the vanes (fig. 1). The exit of the gap between the rotating and fixed cowlings was designed according to the principles suggested in reference 4. The leak gap (fig. 7) was 5/16 inch. Leakage through the gap at the inner spinner was prevented by a sealing plate inside the inner spinner.

INSTRUMENTATION AND TESTS

The internal quantity flow measurements were obtained by the use of three total- and static-pressure rakes installed inside the lip just ahead of the vanes as shown in the sketch of figure 1 and in the photograph of figure 8. The rakes were supported from streamline struts located in the tunnel ahead of the cowling inlet as pictured in figure 9. Each rake contained five total-pressure tubes and four static-pressure tubes.

For the purpose of exploring the boundary layer behind the cowling lip a 3-inch rake containing 10 total-pressure tubes was inserted at the bottom of the annular duct about 10 inches inside the entrance (fig. 1). This rake was installed during preliminary nonrotational tests only.

The leak flow through the spinner-body gap was determined by measurements from three total- and three static-pressure tubes equally spaced around the periphery at station 4 (fig. 1). The angle at which the air left the leak gap was determined from both a yaw tube and tufts installed on the fixed cowling at station 4.

The survey plane at which the total-pressure recoveries were measured is shown as station 5 in figure 1. There were three equally spaced rakes installed, one of which was located at the bottom of the passage; each contained five shielded total-pressure tubes. Inner- and outer-wall static orifices were located adjacent to each rake. Temperatures were measured with thermocouples installed at station 5 and in the tunnel air stream.

Rotational speed was measured with a calibrated aircraft tachometer. The cowling rotated at one-half engine speed. An upper limit to the rotational speed of the cowling of 1200 rpm was maintained as the unbalance caused by the filler increased the centrifugal stresses in the cowling. The engine-cowling flaps were used to regulate the internal-air flow.

The pressure-rise characteristics of this type of cowling at a given angle of attack are defined by the flow coefficient Q_1/nd^3. Each test condition was obtained by operation at constant values of forward and rotational speed and Q_1/nd^3 was varied by changing the cowl-flap setting. Several values of forward and rotational speed were used in order to cover the complete range of operation. All tests were run at a model thrust axis angle of attack of 0°.

RESULTS AND DISCUSSION

Effect of inlet-lip shape.- The pressure recovery measured at station 5 in preliminary tests of the cowling was found to be undesirably low. Boundary-layer measurements 10 inches inside the inlet (fig. 10) indicated that the entering flow was separating from the inner surface of the lip. The balsa filler (fig. 2) was then installed to eliminate this separation. The boundary-layer-survey profiles were used to determine pressure-loss coefficients which represent only the loss due to the boundary layer on the outer passage wall. This average loss is shown as a function of $(V_1/V_o)^2$ in figure 11. The slope of the curve increased at an increasing rate with $(V_1/V_o)^2$ for the original lip, but with the balsa filler installed the variation was nearly linear which is compatible with normal unseparated internal-loss characteristics.

All the data presented herein except that shown in figures 10 and 11 were obtained only for the configuration with the balsa filler installed on the cowling lip.

Pressure surveys behind vanes.- Several representative distributions of pressure coefficient across the annulus at the survey plane (station 5) are given in figure 12 for the range of flow coefficient Q_1/nd_3^3 investigated. The root-mean-square diameter of the passage at station 3 (d_3 = 3.30 feet) was selected as a representative dimension to be used in computing the flow parameter. Each of the local total-pressure coefficients represents the average from three tubes equally spaced around the periphery. These plots reveal that an outwardly increasing total-pressure gradient existed throughout the Q_1/nd_3^3 range. The total-pressure gradient was steepest and a tendency toward flow separation occurred at low values of Q_1/nd_3^3 which correspond to high vane angles of attack, high pressure rise, and high centrifugal forces. In this flow-coefficient range an area of possibly reversed flow existed, as is indicated by the fact that the total pressure was below the static pressure.

Pressure rise through the cowling.- The total pressure available behind the vanes depends upon the pressure rise provided by the vanes and the losses in the cowling. The variation of pressure recovery $\frac{H_5 - p_o}{q_o}$ with $\frac{Q_1}{nd_3^3}$ is given in figure 13 for operating conditions of constant forward and rotational speeds. The pressure recoveries represent the averages, weighted on the basis of $\left(\frac{r}{R}\right)^2$, of the local recoveries across the annulus. The deviation from straight lines shown on some of the curves resulted from operation of the vanes in the stalling region with a consequent loss in pressure rise. The inlet-velocity ratio varied throughout the Q_1/nd_3^3 range for each curve of constant operating condition.

The data of figure 13 were cross-plotted and are given in figure 14 as the variation of pressure recovery with Q_1/nd_3^3 for several constant values of inlet-velocity ratio. As indicated by the curves, the value of Q_1/nd_3^3 of about 0.63, where the pressure recovery is unity, represents the operating condition at which the cowling vanes provided sufficient pressure rise to overcome all losses in the internal-flow system up to station 5. At values of Q_1/nd_3^3 less than 0.63 the vanes operated at positive angles of attack so that the combined pressure rise

due to the vanes and the ram pressure recovered by the cowling was greater than the dynamic pressure of the free stream. Conversely, at values of Q_1/nd_3^3 greater than 0.63 the vanes operated at reduced angles of attack and were not capable of overcoming the pressure losses in the internal flow.

The relationship between the pressure coefficient and pressure recovery is, $\frac{H_5 - H_o}{q_1} = \left(\frac{V_o}{V_1}\right)^2\left(\frac{H_5 - p_o}{q_o} - 1\right)$. Therefore, all of the data given in figure 13 can be shown as a single curve of the nondimensional blower-performance parameters $\frac{H_5 - H_o}{q_1}$ and $\frac{Q_1}{nd_3^3}$ if the losses and pressure rise are constant functions of q_1. This relationship, which eliminates V_1/V_o as a basic variable, is given in figure 15.

Prediction of pressure rise.- In order to predict the pressure rise of a rotating cowling, it is necessary to establish the theoretical pressure rise and the internal aerodynamic losses. The equation for the ideal pressure rise may be obtained if certain assumptions are made in regard to the cowling geometry. The concept of the mean effective diameter used herein represents the root-mean-square diameter of the annulus area at the trailing edge of the vanes. This diameter divides the annular passage into two areas of equal mass flow if the velocity and density distributions are uniform at this station. The equation for the ideal pressure rise of a blower (reference 8) is

$$\Delta H = \rho\omega\left(r_3u_3 - r_2u_2\right)$$

When there is no prerotation of the air at the inlet, $u_2 = 0$. Therefore, the equation may be expressed in terms of the rotational velocities at the vane outlet:

$$\Delta H = \rho U_3u_3$$

where the rotational velocity of the vane $U_3 = r_3\omega = \pi nd_3$.

The vector diagram of velocities at the vane trailing edge (station 3) is shown in figure 16. The rotational velocity of the air

is $u_3 = \pi n d_3 - V_{a_3} \tan \theta$. The pressure rise may be written as a pressure coefficient:

$$\frac{H_3 - H_o}{q_1} = \frac{\rho \pi n d_3 u_3}{\frac{1}{2}\rho V_1^2}$$

The velocity at the inlet (station 1) may be expressed in terms of the inlet flow Q_1 and area A_1. Thus the pressure-rise coefficient becomes:

$$\frac{H_3 - H_o}{q_1} = \frac{2\pi n d_3 \left(\pi n d_3 - V_{a_3} \tan \theta\right)}{(Q_1/A_1)^2}$$

In terms of the flow coefficient

$$\frac{H_3 - H_o}{q_1} = \frac{\dfrac{2A_1^2\pi^2}{(d_3)^4}}{\left(\dfrac{Q_1}{nd_3^3}\right)^2} - \frac{\dfrac{2A_1^2\pi}{A_3 d_3^2} \tan \theta}{\dfrac{Q_1}{nd_3^3}} \qquad (1)$$

Since the variation of pressure rise with flow coefficient has been established, it is now necessary to determine the manner in which the losses vary with Q_1/nd_3^3. The losses which can be expressed in terms of $\dfrac{H - H_o}{q_1}$ are primarily due to diffuser separation and skin friction. When the vanes operate unstalled it is assumed that the losses can be expressed as a function of the resultant dynamic pressure at the vane leading edge:

$$(\Delta H)_{loss} = k q_r$$

In coefficient form this expression becomes:

$$\frac{(\Delta H)_{loss}}{q_1} = k \frac{\frac{1}{2}\rho V_r^2}{\frac{1}{2}\rho V_1^2}$$

and $V_r^2 = \left(\frac{Q_1}{A_{LE}}\right)^2 + (\pi n d_{LE})^2$ where d_{LE} is the root-mean-square diameter of the passage at the vane leading edge. In terms of flow coefficient, the loss coefficient may be written thus:

$$\frac{(\Delta H)_{loss}}{q_1} = k\left[\frac{\frac{(\pi d_{LE} A_1)^2}{d_3^6}}{\left(Q_1/nd_3^3\right)^2} + \left(\frac{A_1}{A_{LE}}\right)^2\right] \tag{2}$$

The rotating-cowling pressure-rise equation, including the internal aerodynamic losses, is now written:

$$\frac{H_3 - H_o}{q_1} = \frac{\frac{2A_1^2\pi^2}{(d_3)^4}}{\left(\frac{Q_1}{nd_3^3}\right)^2} - \frac{\frac{2A_1^2\pi}{A_3 d_3^2}\tan\theta}{\frac{Q_1}{nd_3^3}} - k\left[\frac{\frac{(\pi d_{LE} A_1)^2}{d_3^6}}{\left(\frac{Q_1}{nd_3^3}\right)^2} + \left(\frac{A_1}{A_{LE}}\right)^2\right] \tag{3}$$

Comparison of calculated and experimental pressure rise.- For the present cowling, $A_1 = 2.57$ square feet, $d_3 = 3.30$ feet, $A_3 = 5.03$ square feet, $d_{LE} = 1.82$ feet, and $A_{LE} = 1.68$ square feet = the area at the vane leading edge taken normal to the cowling axis. Substituting these values in equation (3) gives the pressure-rise equation for this cowling.

$$\frac{H_3 - H_o}{q_1} = \frac{1.107}{\left(\frac{Q_1}{nd_3^3}\right)^2} - \frac{0.760\tan\theta}{\frac{Q_1}{nd_3^3}} - k\left[\frac{0.169}{\left(\frac{Q_1}{nd_3^3}\right)^2} + 2.34\right] \tag{4}$$

The quantities θ and k in equation (4) are unknown for the present cowling. Evaluation of these quantities is necessary in order to compare the theoretical pressure-rise coefficients with the measured values. In flows of this type where the passages are long and narrow and the vane trailing edges are straight and thin, the exiting flow necessarily leaves in a fixed direction, that is, roughly parallel to the vane mean line at the trailing edge, regardless of the relative direction of the entering air. For such cases θ would be constant and, furthermore, its value would be determined by the vane geometry. In the present cowling, however, it is not obvious that θ would be constant, and even if it were, its value would not be evident because of the thick rounded trailing edge. The loss factor k also is probably not constant, since it should depend to some extent on the relative alinement of the incoming air with the vane leading edge.

In order to determine, however, whether the concept of a constant θ and k was roughly in agreement with experiment, curves obtained from equation (4) were plotted for three fixed values of k, (k = 0.1, 0.3, and 0.5) and three fixed values of θ, ($\theta = 50^\circ$, 55°, and 60°) where the value $\theta = 55^\circ$ corresponds to the condition at which the exiting flow is parallel to the vane mean line at the trailing edge. These curves are compared with the experimental curve in figure 17. The general agreement in shape between the calculated and experimental curves indicates that an analysis along such lines is satisfactory. The fact that the experimental curve is rotated somewhat with respect to the calculated curves is possibly due to improvement in the alinement of the entering flow, and corresponding improvement in internal flow, with increasing Q_1/nd_3^3. Such improvement would cause not only a reduction of k, but also, because of the reduced separation on the downstream face of the vane, a simultaneous reduction of θ. For example, at a θ of 55°, a change of about 0.15 in k, or simultaneous changes of about 0.1 in k and about 3° in θ, across the given Q_1/nd_3^3 range would account for the indicated differences between the calculated and experimental curves.

A second reason for the discrepancy between the slopes of the calculated and experimental curves results from the method of averaging the pressures. If sufficient measurements had been obtained to permit weighting the local total pressures with respect to mass flow instead of area, the average total-pressure coefficients in the low Q_1/nd_3^3 range would have been larger than the values given, while the coefficients in the higher Q_1/nd_3^3 range would have been increased to a smaller extent. A further rotation of the experimental curve in the direction closer to the calculated curves would be obtained if the total pressure of the flow leaving the leakage gap could have been taken into account in the averaging process.

Leak flow.- A characteristic of the rotating cowling is that part of the air flow through the inlet is lost at the leak gap and the useful quantity flow available at the propulsion unit is thereby reduced. The magnitude of the leak flow is a function of various flow parameters as well as the geometry of the leak gap. The effects of several types and sizes of gaps on the leak flow are given in reference 5. A leak gap designed to provide a flow passage of minimum aerodynamic loss is described in reference 4.

The leak gap used with the present cowling is shown on figure 7 and the following results apply only to this type of gap. The leak flow was measured at station 4 just inside the gap where the total pressure, static pressure, and angle measurements were obtained and the gap area was known.

The ratio of the total pressure measured at station 4 to the average of the pressures indicated by the three outer tubes located at station 5 varied from 0.97 to 1.00 throughout the entire range of test conditions. The low total-pressure losses through the gap indicate that the present gap design is satisfactory.

The variation of leak flow with inlet quantity flow for several operating conditions is presented in figure 18. For a constant inlet flow and rotational speed, the leak flow increased with increasing forward speed mainly because of the reduced external pressure near the leak exit. At constant inlet flow and forward speed, the leak flow increased with increasing rotational speed as a result of greater internal pressure provided by the vanes.

The effect of the flow parameters on the leak flow is given in figure 19. At low values of inlet-velocity ratio and Q_1/nd_3^3 the flow escaping through the leak gap amounted to more than 25 percent of the total inlet flow for this particular cowling configuration. At high values of Q_1/nd_3^3 the variation of the quantity Q_L/Q_1 was small for a constant inlet-velocity ratio.

The leak-flow quantity has been calculated from the expression

$$Q_{L_{calc}} = A_4\sqrt{\frac{2(H_5 - p_s)}{\rho}}$$

where p_s is the local static pressure on the cowling surface at the station corresponding to the position of the leak gap and was determined from the data of reference 9 for a nonrotating continuous cowling and

$\bar{\rho}$ is the average of the densities at station 5 and at the cowling surface at the leak gap. The variation of the measured leak flow with the calculated flow is shown in figure 20. The points fall on a single straight line, the slope of which is the leak-gap-orifice coefficient. The value of the coefficient

$$C = \frac{Q_L}{Q_{L_{calc}}} = \frac{A_4\left[\sqrt{\frac{2(H_4 - p_4)}{\rho_4}}\right]\cos\psi}{A_4\sqrt{\frac{2(H_5 - p_s)}{\bar{\rho}}}}$$

was found to be 0.66.

For the purpose of estimating the leak flow for a rotating cowling having a similar leak-gap design the following equation may be used:

$$Q_L = 0.66A_4\sqrt{\frac{2(H_5 - p_s)}{\bar{\rho}}}$$

The value of H_5 can be obtained from the calculated pressure-rise characteristics of the rotating cowling. The surface static pressure can be determined from the data of reference 9. The average density $\bar{\rho}$ can be estimated from the external density and the internal-flow conditions; usually the pressure rise through the vanes is small for the design condition. Since the pressure-rise range for this type of cowling will be small, it may be assumed that the density will be constant over the operating range. The assumptions involved in the foregoing method will result in a relatively small error in estimation of the leak flow. The effect of such errors on the over-all pressure-rise characteristics of the cowling will be still less since the leak flow will be only a portion of the total inlet quantity flow. This is especially true of installations for gas-turbine engines which require a much greater quantity flow than the present engine installation.

Design considerations.- The procedure for designing a rotating cowling for a specified propulsion unit involves several features which are not encountered with fixed cowlings. A general approach to these design problems is therefore discussed in the following paragraphs.

The performance requirements of the airplane and the selected engine-propeller combination establish the propulsion-unit mass flow, the cowling rotational speed, and the desired engine inlet pressure.

With these quantities known, the internal aerodynamic problems which arise include an evaluation of the leak-flow quantity, determination of the internal-flow losses, and the design of the vanes.

A layout of the propulsion system will provide the preliminary over-all dimensions necessary for the selection of a cowling. From this information and the knowledge of internal-air flow obtained from both the engine mass flow and the leakage flow estimated from data such as are given in figure 19, a cowling external shape may be selected through the use of design charts such as those given in reference 9.

If this shape and the desired pressure behind the vanes is utilized, the leak flow may then be determined more accurately by the method outlined in the section entitled "Leak flow." The revised inlet quantity flow may necessitate a reselection of the external cowling proportions and the design inlet-velocity ratio. It should be pointed out that, if the resulting inlet-velocity ratio is high, the advantages of a rotating cowling are diminished.

The layout of the engine-propeller combination will determine the coordinates of the inner spinner. The general shape of the internal passage will depend upon the spinner dimensions and the desired velocity at the engine inlet as well as the area variation required to minimize the losses through the annulus. The root-mean-square passage diameter at the rear of the rotating portion of the cowling may then be determined and the design Q_1/nd_3^3 may be calculated. With this passage geometry the internal aerodynamic losses in the rotating portion of the cowling may be estimated for some value of Q_1/nd_3^3. In the case where the diffusion is zero or small, the magnitude of the losses may be estimated by calculating the skin friction. The value of the loss coefficient k may then be determined from equation (2).

The approximate vane geometry is determined by the shape of the propeller shanks and the resultant air path in the rotating cowling. It should be pointed out that the air follows an expanding helical path with respect to the rotating cowling and the local values of Q_1/nd^3 vary through the cowling. The geometry may be used to evaluate the constants in equation (3) which can then be solved to determine the air angle θ. The difference between this θ and the corresponding angle of the air helix at station 3 represents the increase in angle of attack at which the vane must operate in order to overcome the losses in the rotating passage. If it is desired that free-stream total pressure be made available at the face of the engine, an increment in vane setting may be necessary to provide added pressure rise to overcome the losses in the fixed portion of the cowling. An additional correction to the angle θ arises from an alteration in the direction of the vector W_3 which is due to the mutual blade interference occurring in cascades.

The magnitude of this correction cannot be determined at this time. A rough estimate based on cascade studies which may or may not be applicable indicates that the trailing edge should be turned 3° to 5° past the desired direction of the outgoing flow. The position of the vane may then be determined by assuming that the air helix represents the vane mean line which may be rotated to allow for all the angle-of-attack corrections. Area compensation for vane blockage may be accomplished by adjustment of the passage walls. The utilization of camber instead of increased angle-of-attack corrections should also be considered as a means of providing the necessary pressure rise.

CONCLUDING REMARKS

An experimental and analytical investigation was conducted to study the pressure-rise and leakage-loss characteristics of rotating cowlings. A method for determining the pressure-rise characteristics of this type of cowling has been derived.

The pressure-rise characteristics of the test cowling were investigated over a broad range of the internal-flow parameters. A comparison of the experimental and analytical results indicates that the pressure-rise characteristics can be predicted if the internal losses and the flow angle at the vane trailing edge are known.

The total-pressure losses through the leak gap were of negligible magnitude for all conditions investigated. The flow lost through the leak gap varied from about 5 percent to more than 25 percent of the inlet quantity flow. The leakage flow was greatest at low inlet-velocity ratios and high values of vane pressure rise.

Some of the features peculiar to the design of rotating cowlings are discussed and methods for estimating the leakage losses and the proper vane setting are outlined.

Langley Aeronautical Laboratory
National Advisory Committee for Aeronautics
Langley Air Force Base, Va.

REFERENCES

1. McHugh, James G.: Progress Report on Cowlings for Air-Cooled Engines Investigated in the NACA 19-Foot Pressure Wind Tunnel. NACA ARR, July 1941.

2. Becker, John V.: Wind-Tunnel Tests of Air Inlet and Outlet Openings on a Streamline Body. NACA ACR, Nov. 1940.

3. Biermann, David, and Turner, L. I., Jr.: Ground-Cooling and Flight Tests of an Airplane Equipped with a Nose-Blower Engine Cowling. NACA ACR, Oct. 1939.

4. Becker, John V., and Mattson, Axel T.: The Effect of Spinner-Body Gap on the Pressures Available for Cooling in the NACA E-Type Cowling. NACA CB, March 1943.

5. Seddon, J., Mullins, M. F., and Harper, D. J.: Wind Tunnel Model Tests on the Cooling and Drag Characteristics of Two Hollow Spinner Fans, Suitable for a Radial Air-Cooled Engine, or an Annular Ring Radiator, Mounted behind a Tractor Propeller. Rep. No. Aero. 2085, British R.A.E., Oct. 1945.

6. Anderson, Harris D.: Whirl Test of Hamilton Standard Blower Spinner on an 11-Ft. 3-In. Hydromatic Propeller for Use on an A-20A Airplane. Whirl Test No. 1528. ACTR No. 4715, Materiel Div., Army Air Corps, Dec. 2, 1941.

7. Hild, D. F.: Whirl Test of a Hamilton Standard Blower Spinner, Part No. 55400, on an 11-Ft. 3-In. Hydromatic Propeller. Whirl Test No. 1552, AAFTR No. 4955, Materiel Center, Army Air Forces, June 28, 1943.

8. Eckert, B.: Calculation and Design of Flow Machines in Aircraft Power Plants. Vol. 12, BUSHIPS 338, Navy Dept., May 1946.

9. Baals, Donald D., Smith, Norman F., and Wright, John B.: The Development and Application of High-Critical-Speed Nose Inlets. NACA Rep. 920, 1948.

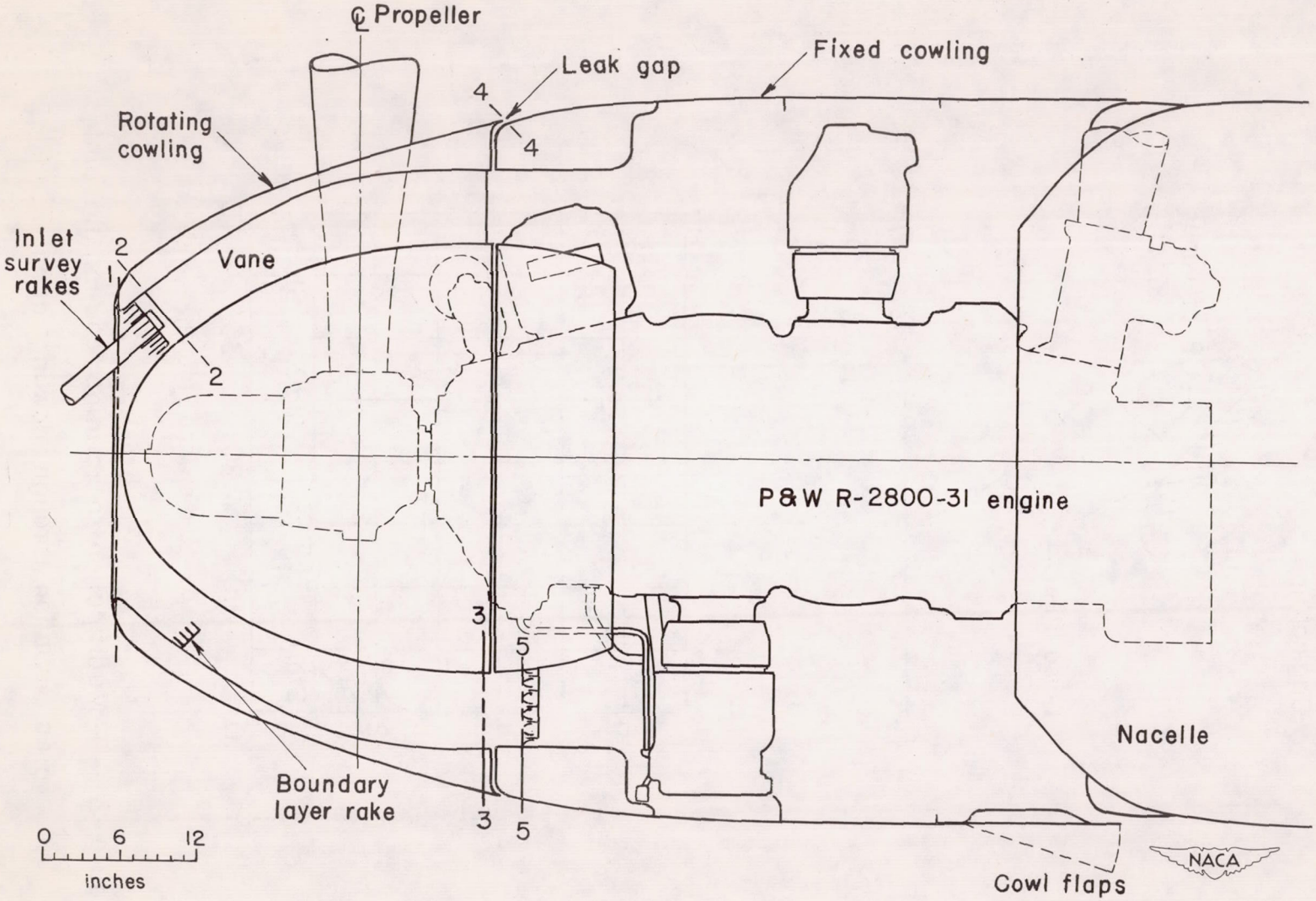

Figure 1.—Sketch of rotating cowling with original lip configuration.

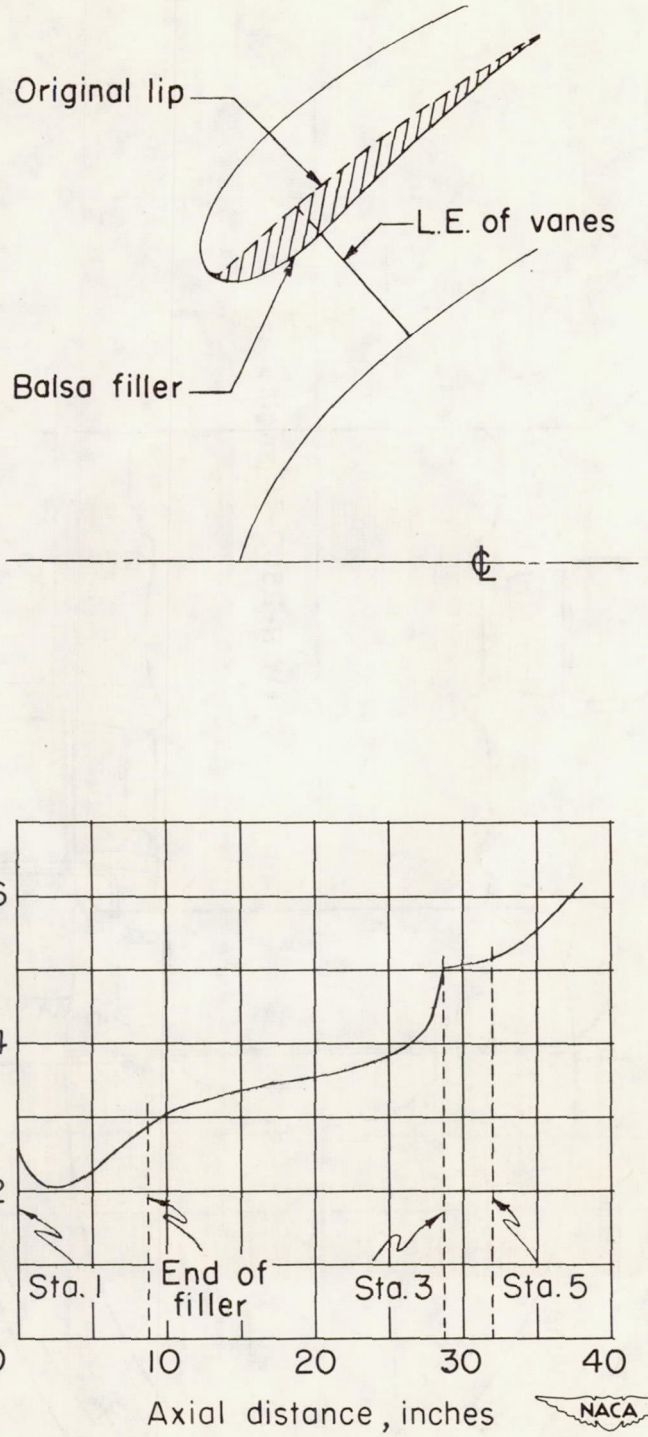

Figure 2. —— Modification to rotating cowling lip and area variation through cowling annulus.

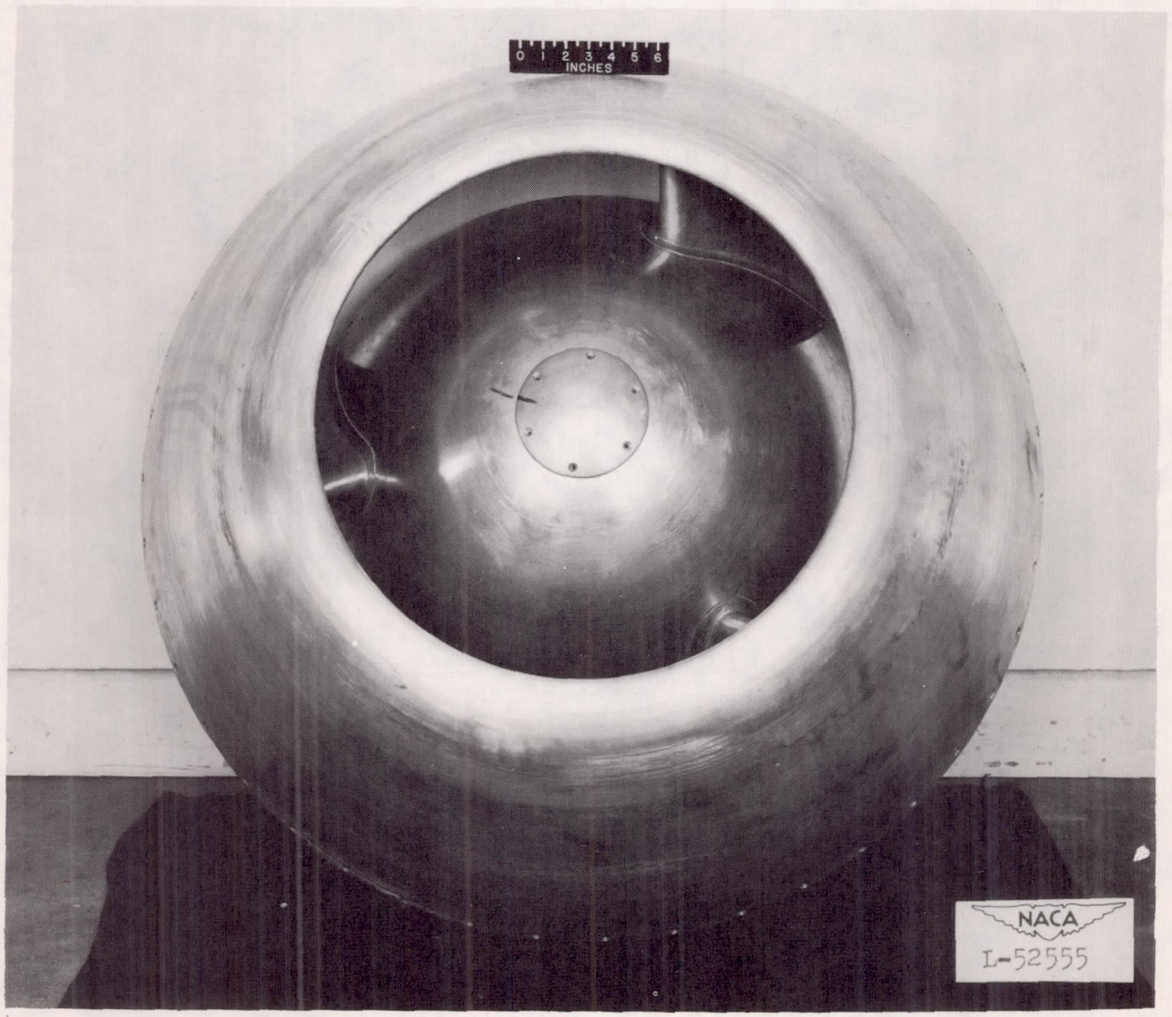

(a) Front view.

Figure 3.- Front section of rotating cowling.

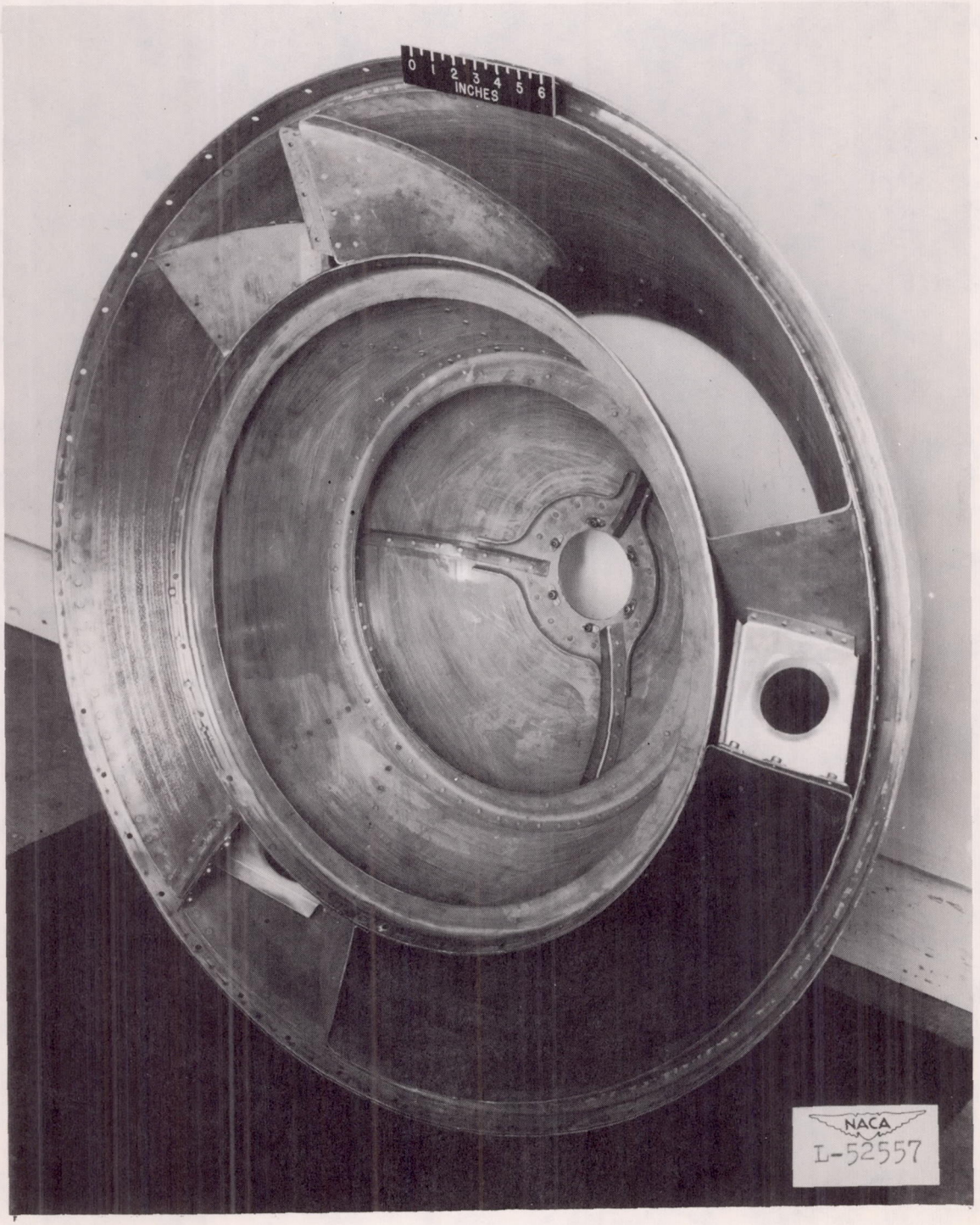

(b) Rear view.

Figure 3.– Concluded.

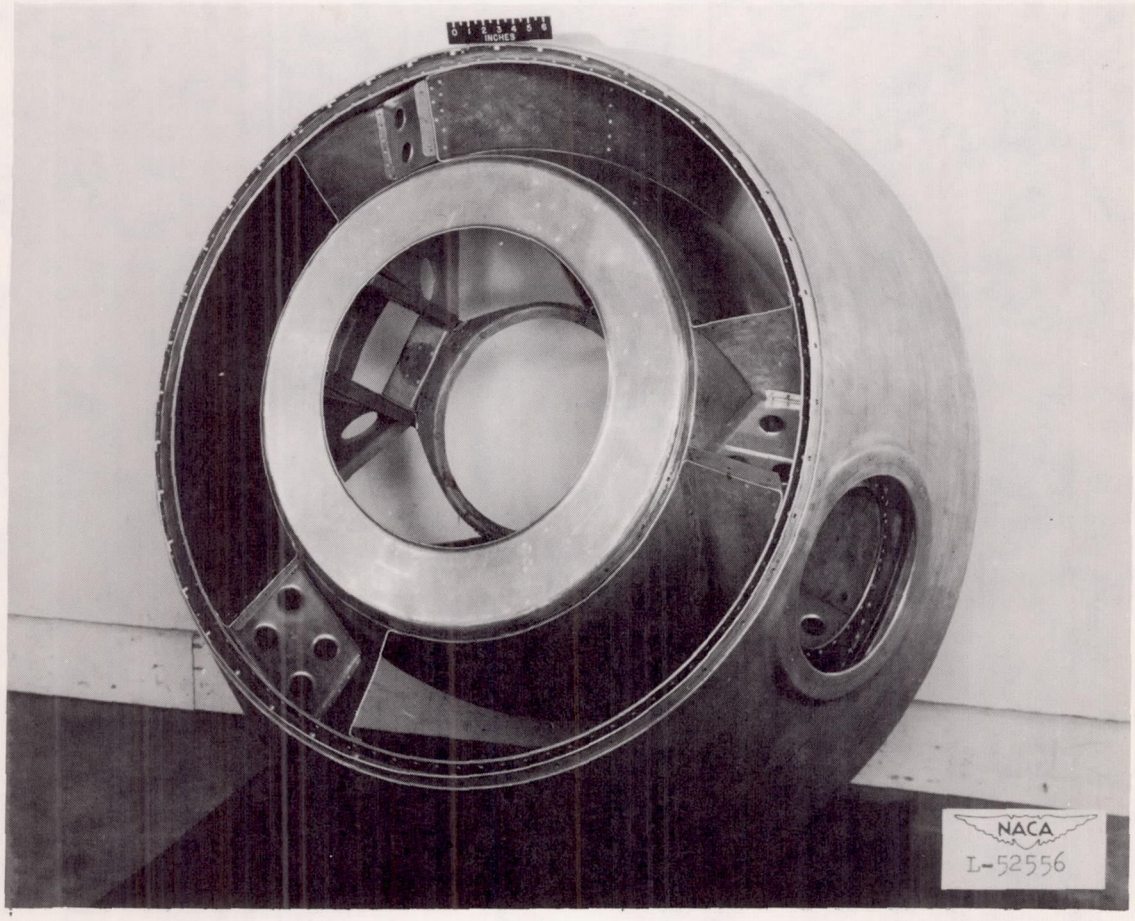

(a) Front view.

Figure 4.– Rear section of rotating cowling.

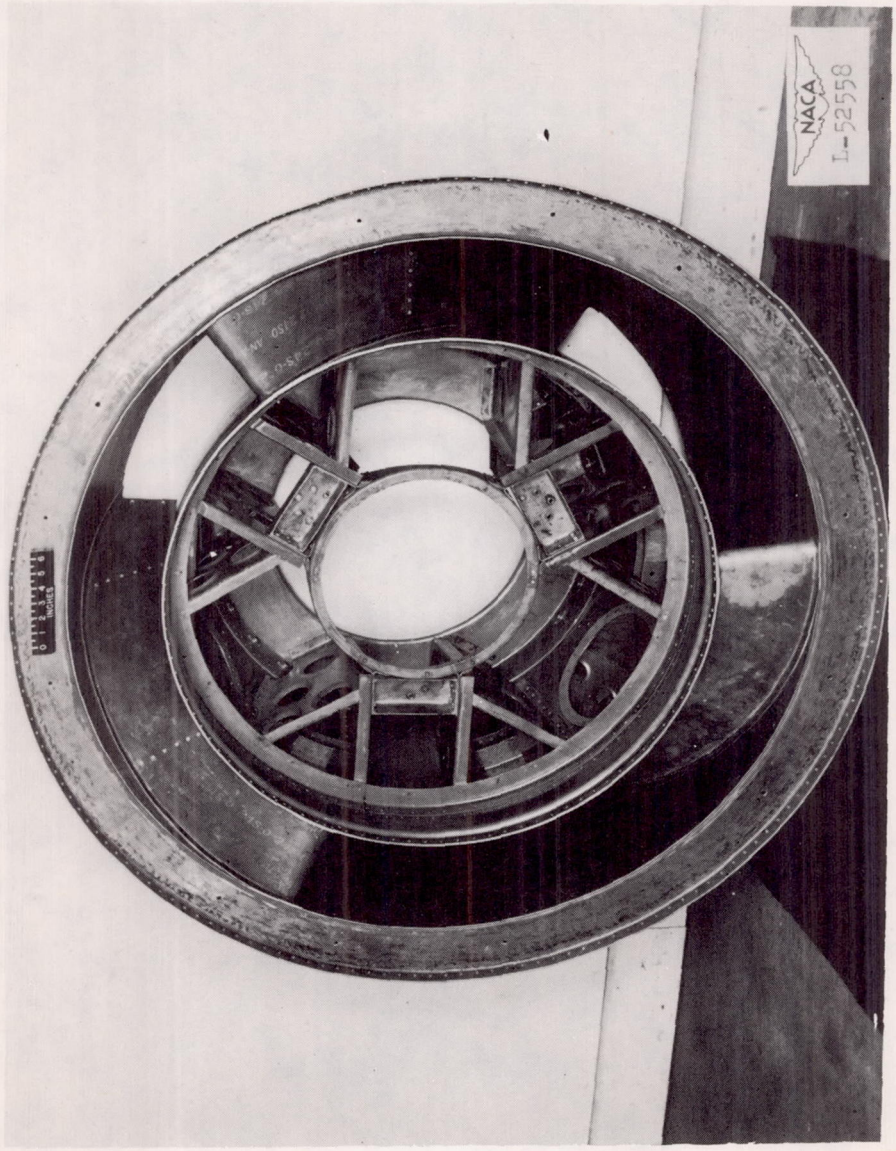

(b) Rear view.

Figure 4.- Concluded.

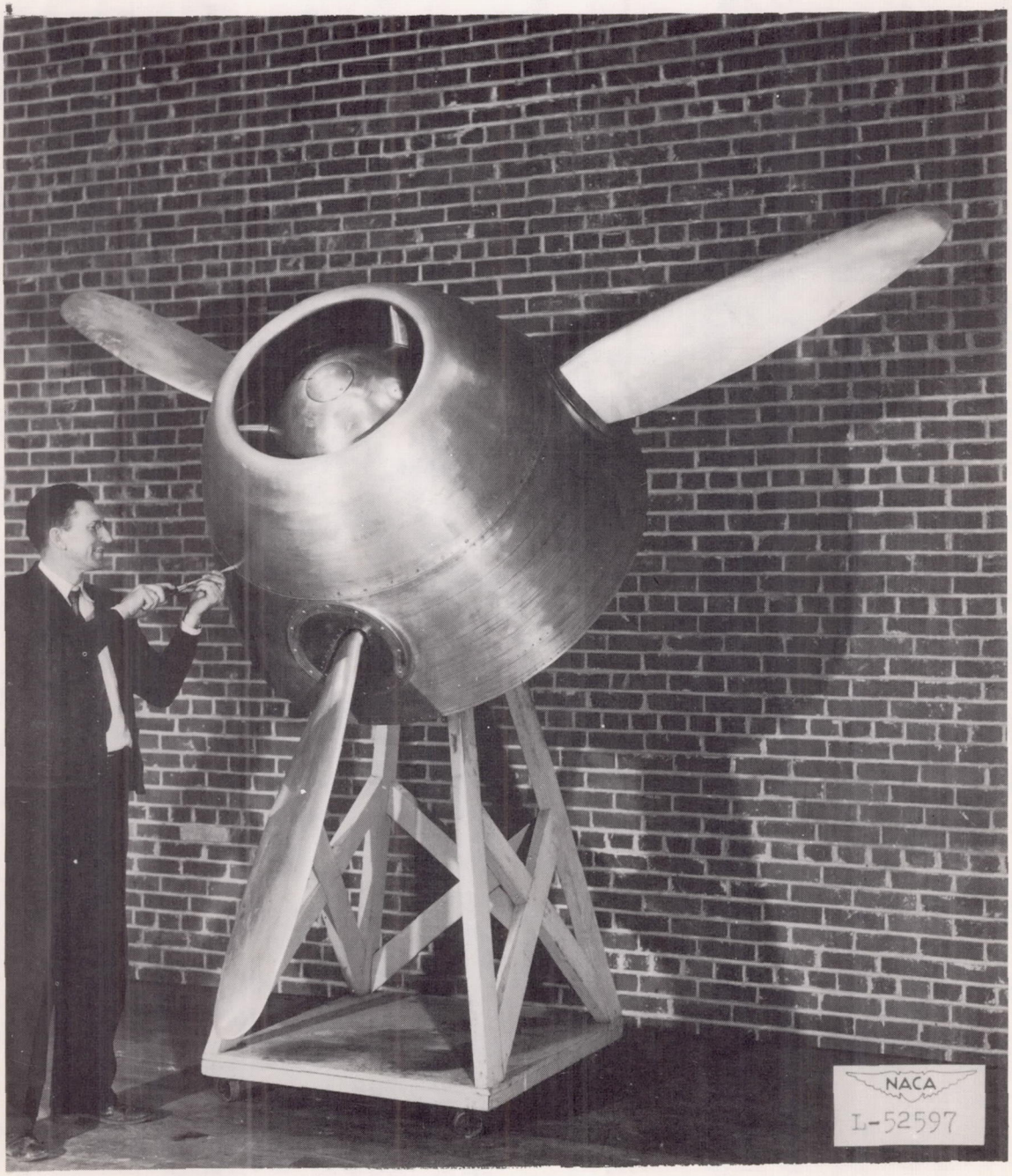

Figure 5.– Rotating cowling and propeller assembly.

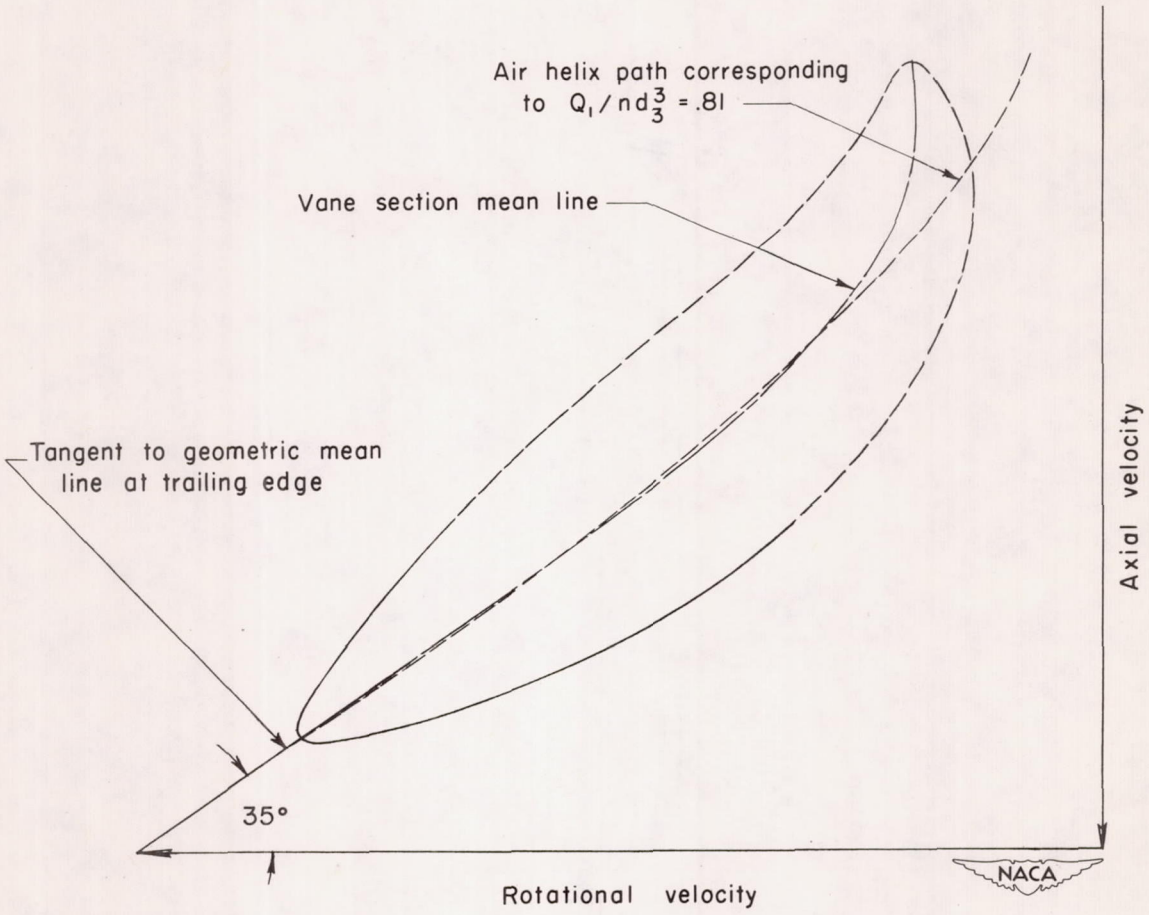

Figure 6.— Diagram representing the vane root-mean-square radius section.

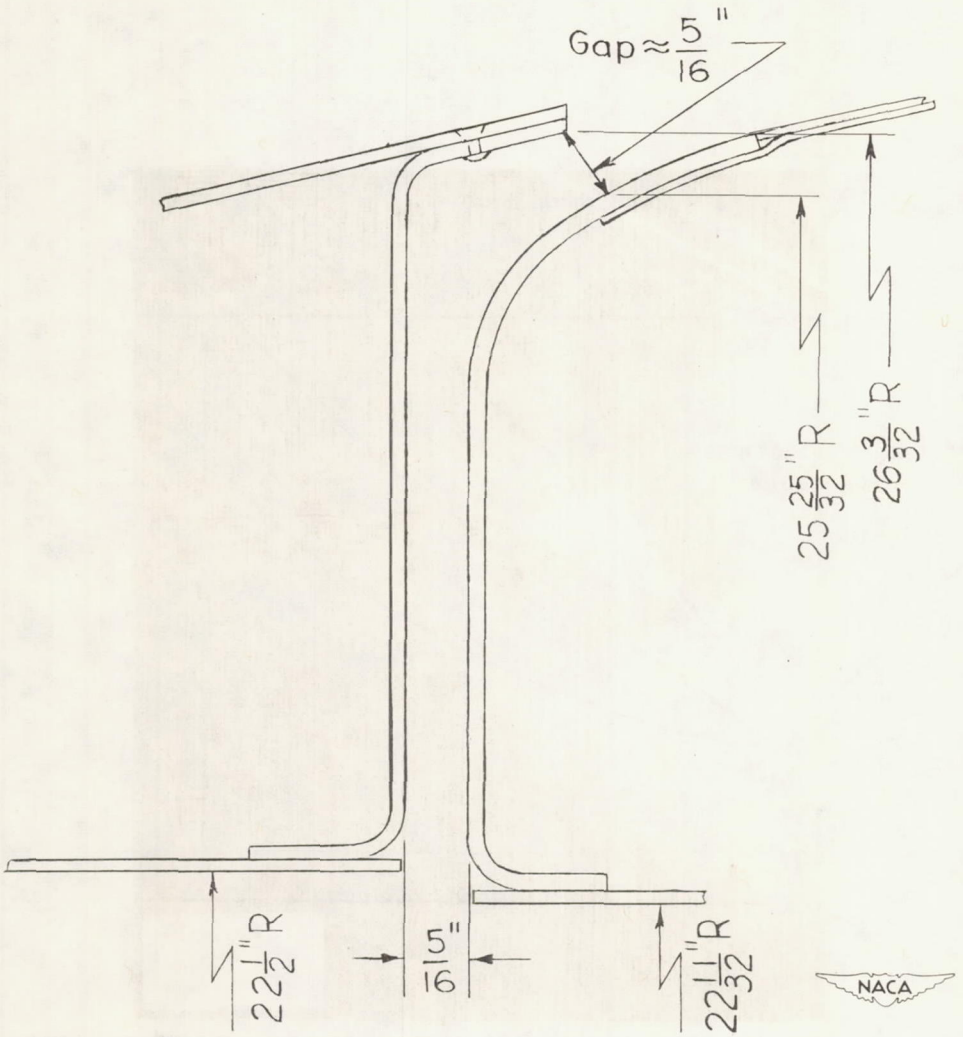

Figure 7.—— Sketch of leak gap.

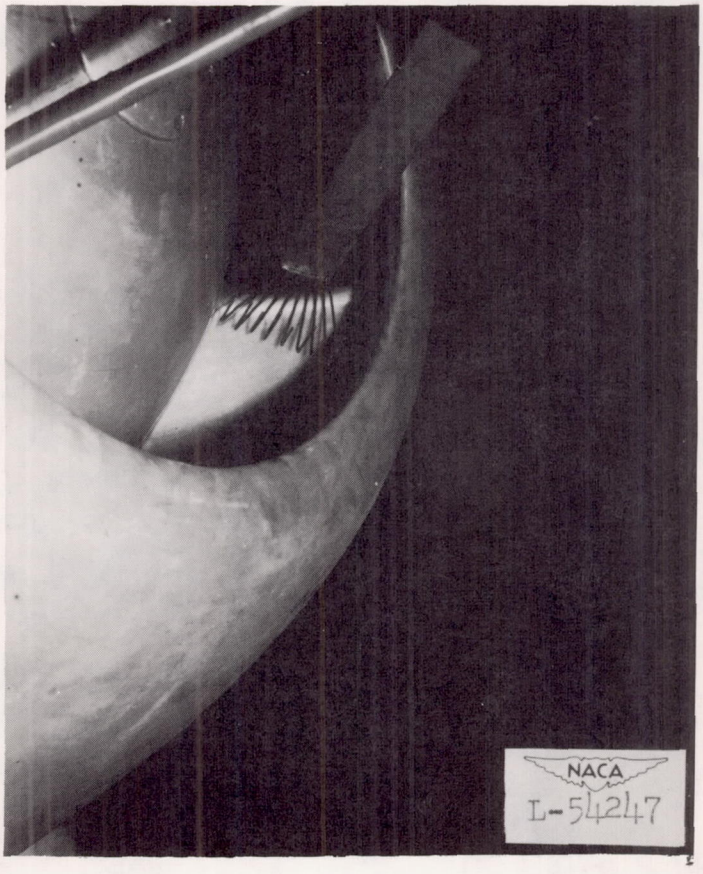

Figure 8.– View of inlet rakes.

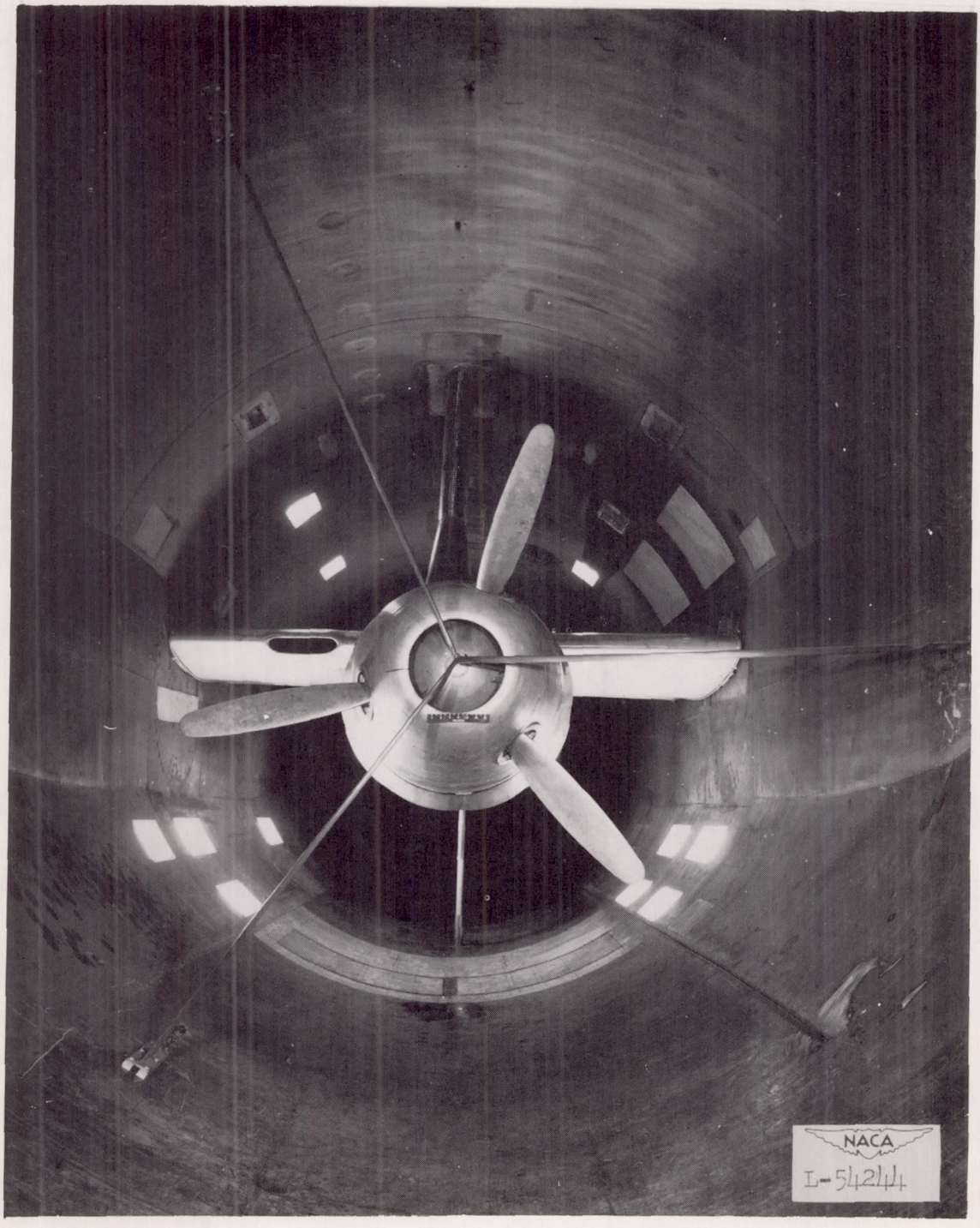

Figure 9.– Rotating cowling installed in tunnel test section.

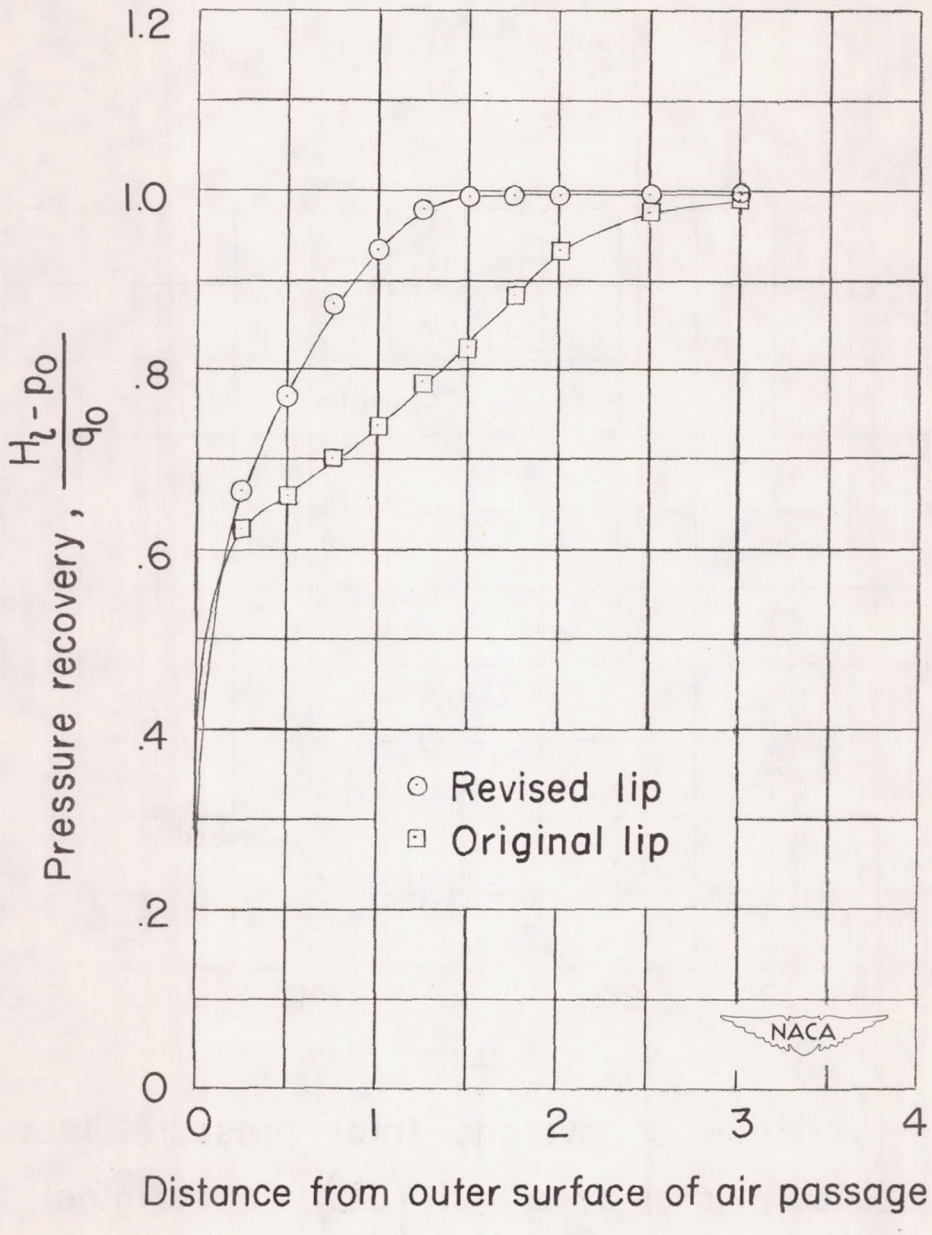

Figure 10.—Boundary-layer profile 10 inches behind rotating cowling inlet. $V_0 \approx 235$ ft./sec.; $V_1 / V_0 \approx 0.56$.

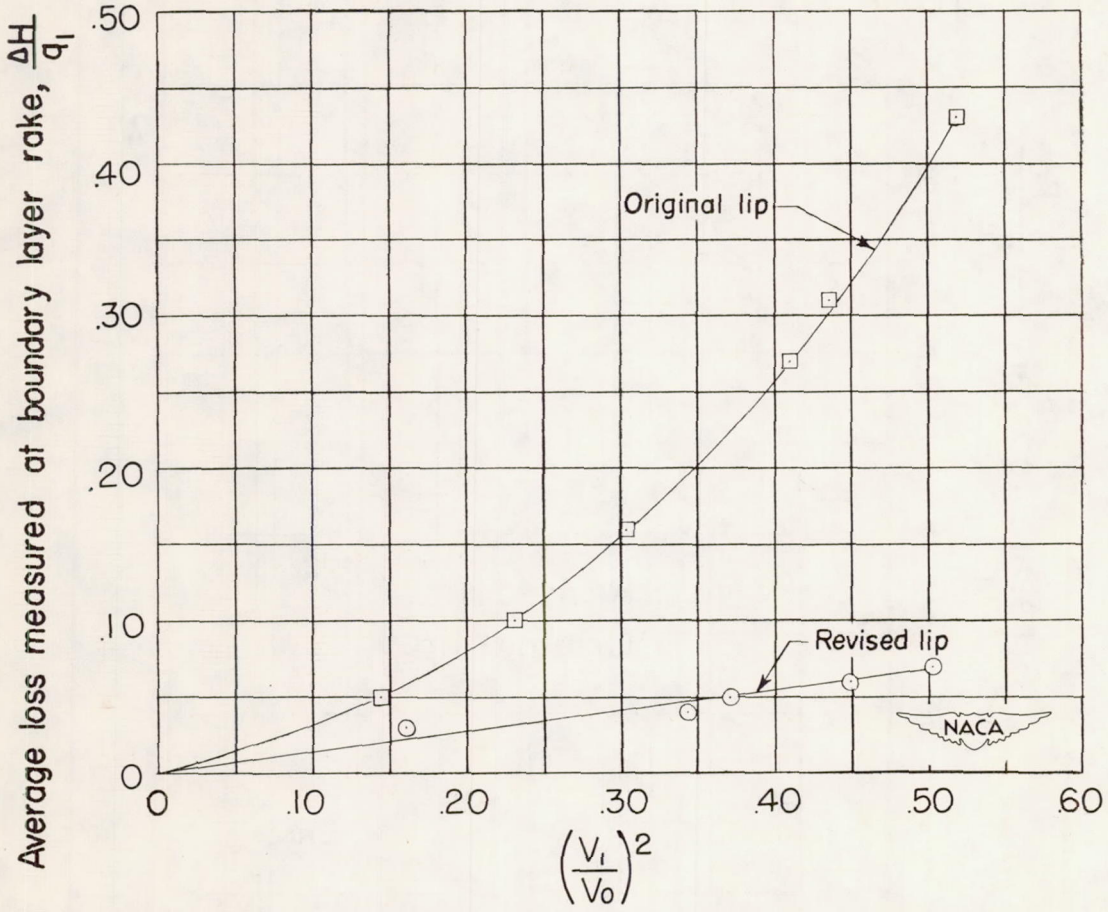

Figure 11.—Variation of average total-pressure loss at boundary layer rake with $\left(\frac{V_1}{V_0}\right)^2$ for original and revised lips.

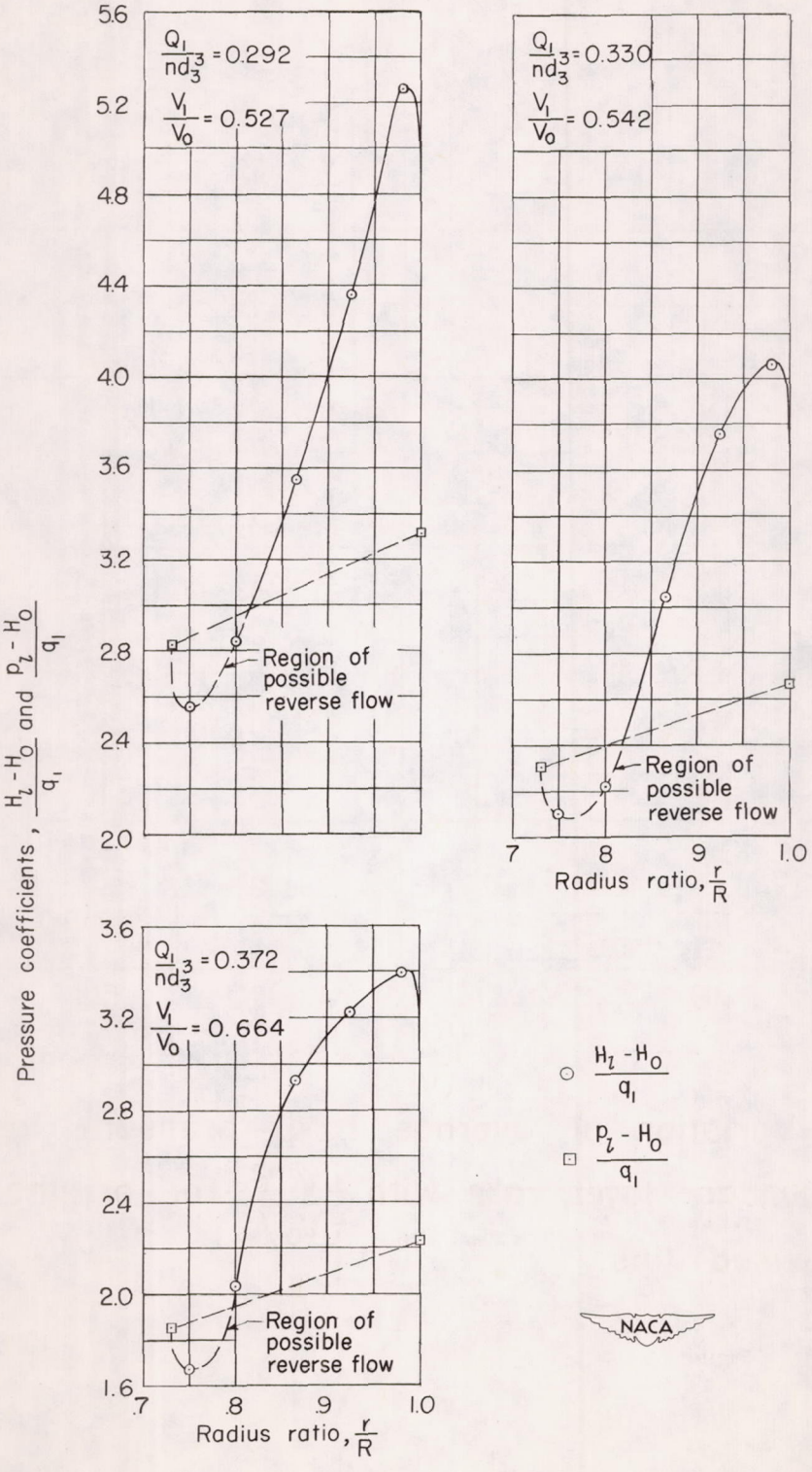

(a) $\frac{Q_1}{nd_3^3} = 0.292$ to 0.372.

Figure 12.— Pressure distribution across annulus at station 5.

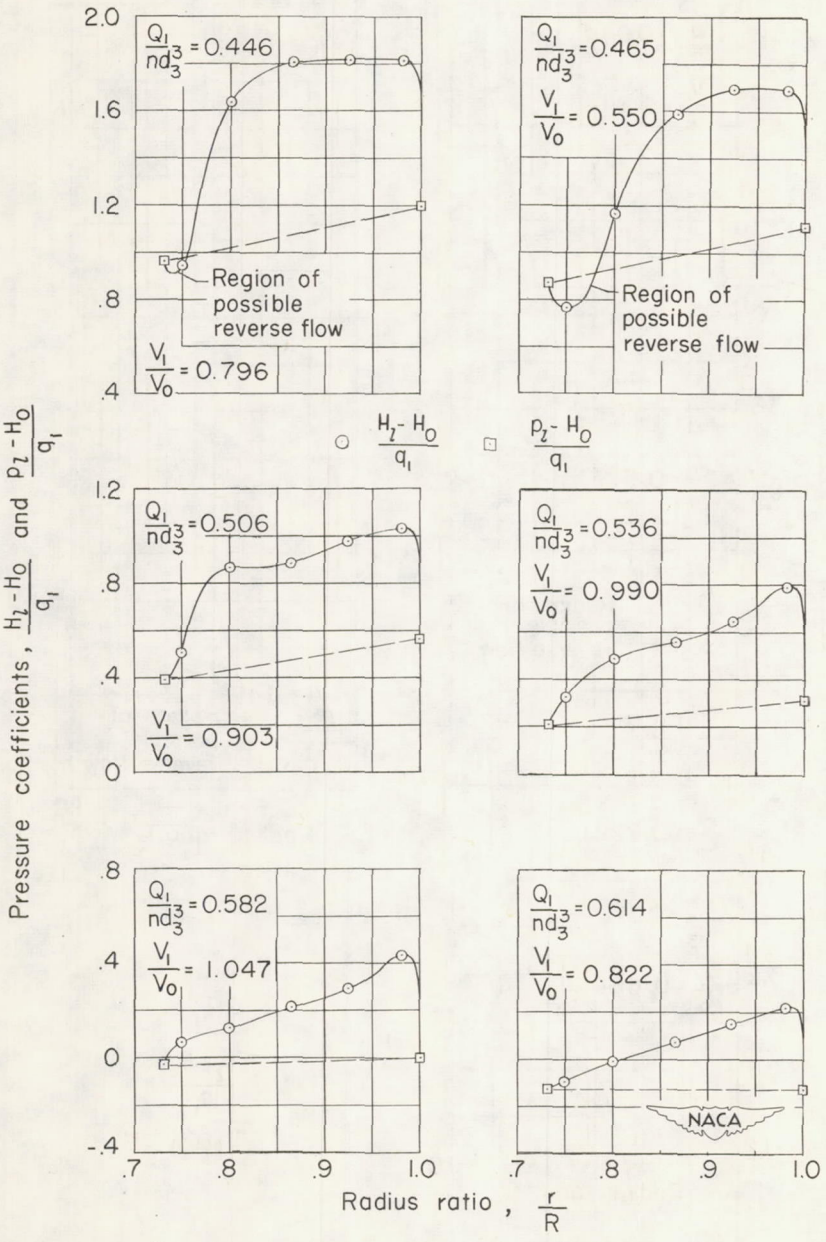

(b) $\frac{Q_1}{nd_3^3} = 0.446$ to 0.614.

Figure 12. — Continued.

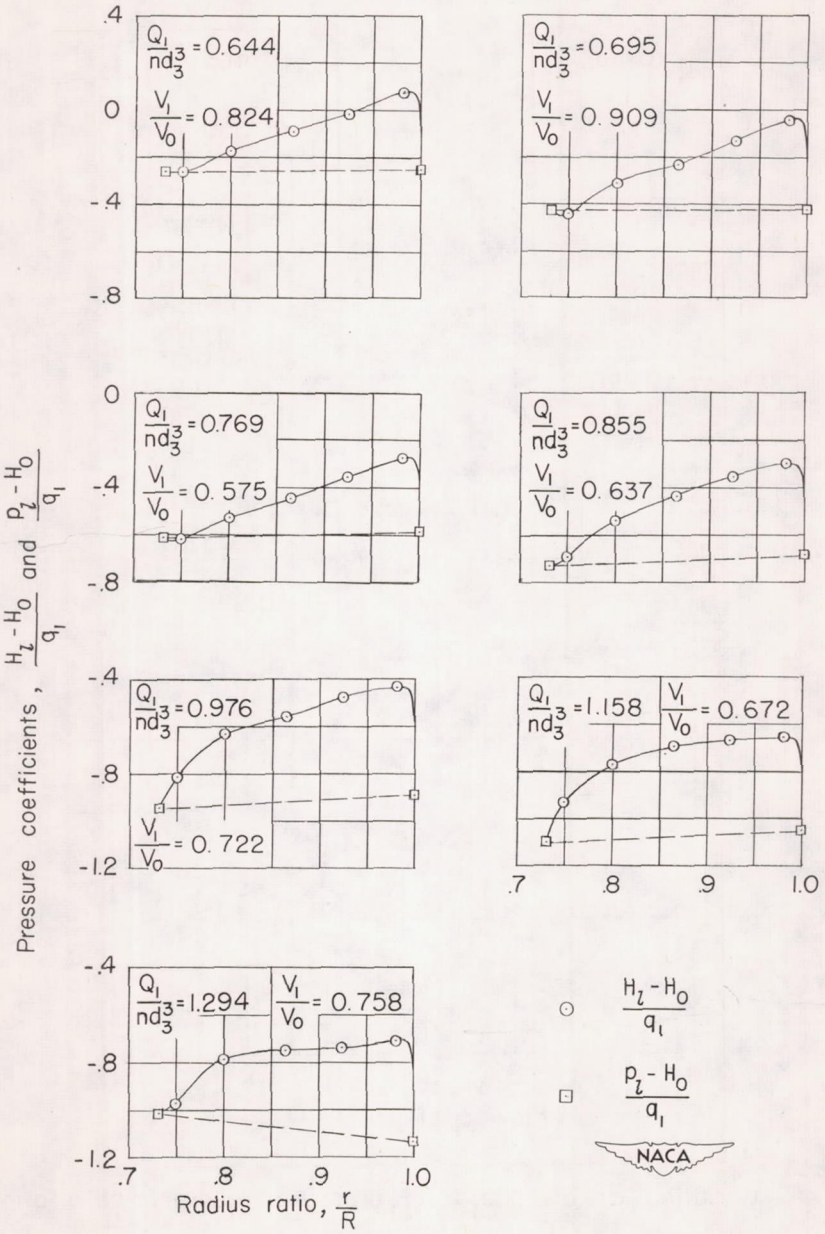

(c) $\frac{Q_1}{nd_3^3}$ =0.644 to 1.294.

Figure 12. — Concluded.

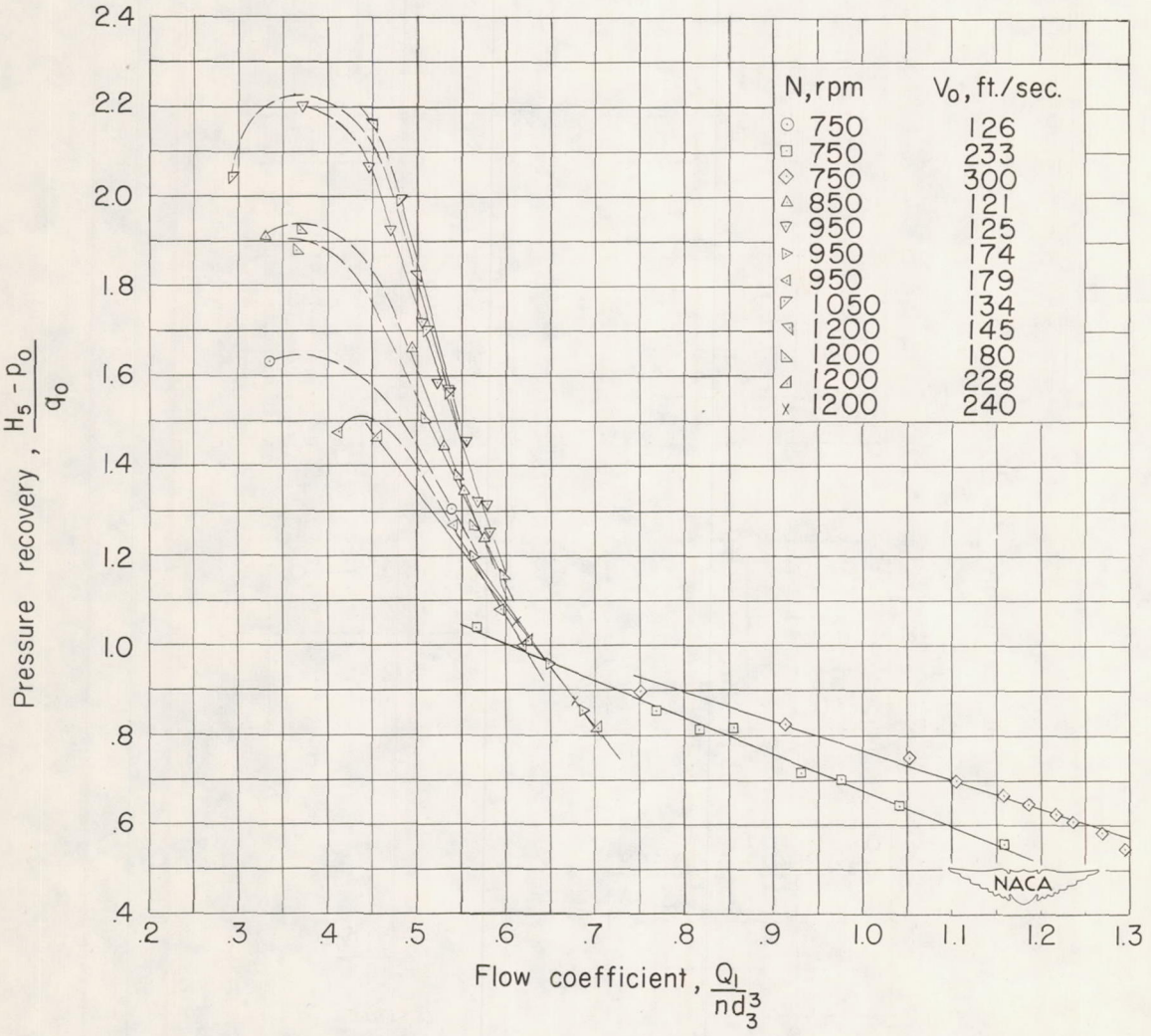

Figure 13. — Variation of average total-pressure recovery at station 5 with flow coefficient.

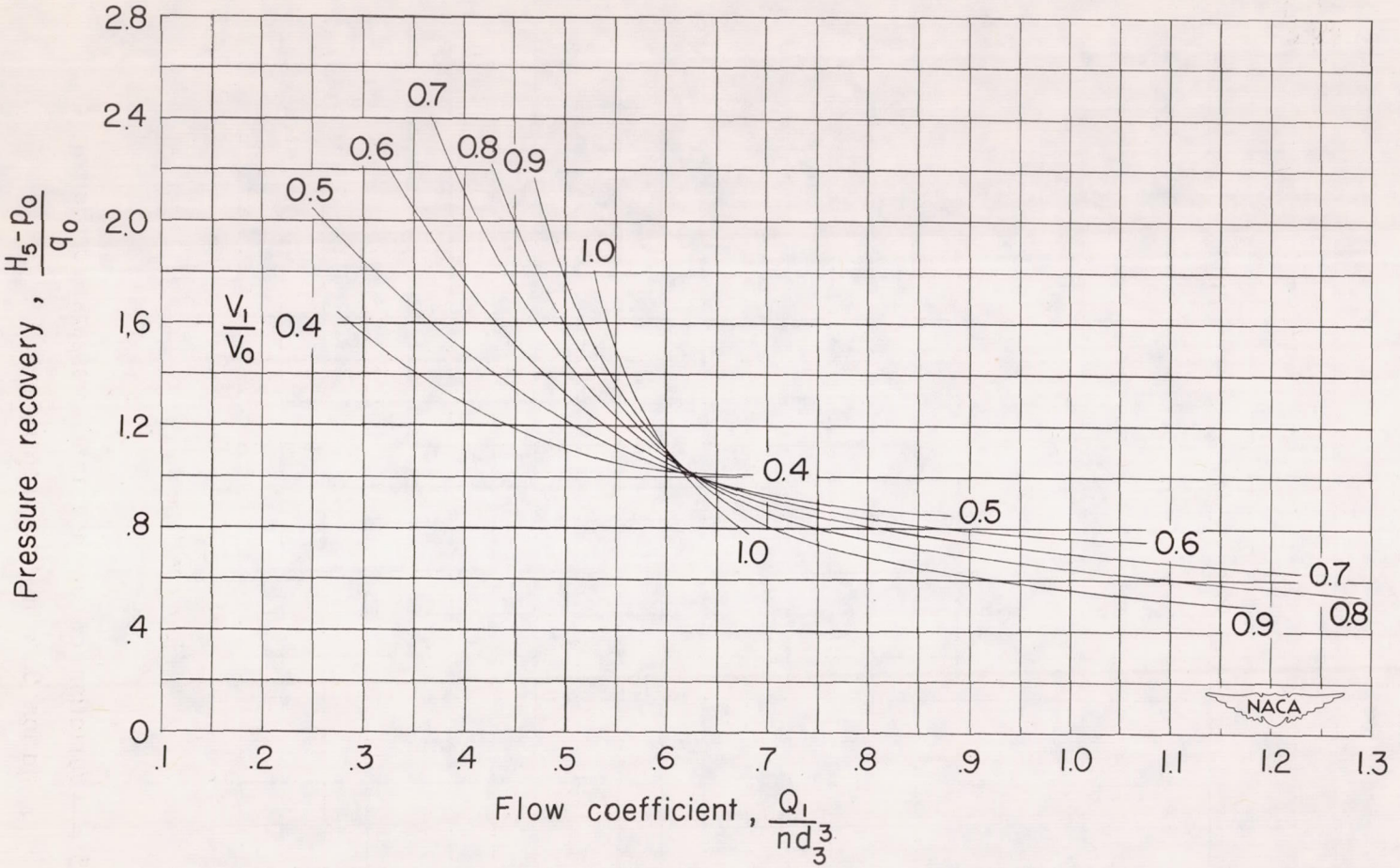

Figure 14.——Variation of average total-pressure recovery at station 5 with flow coefficient for constant values of inlet-velocity ratio.

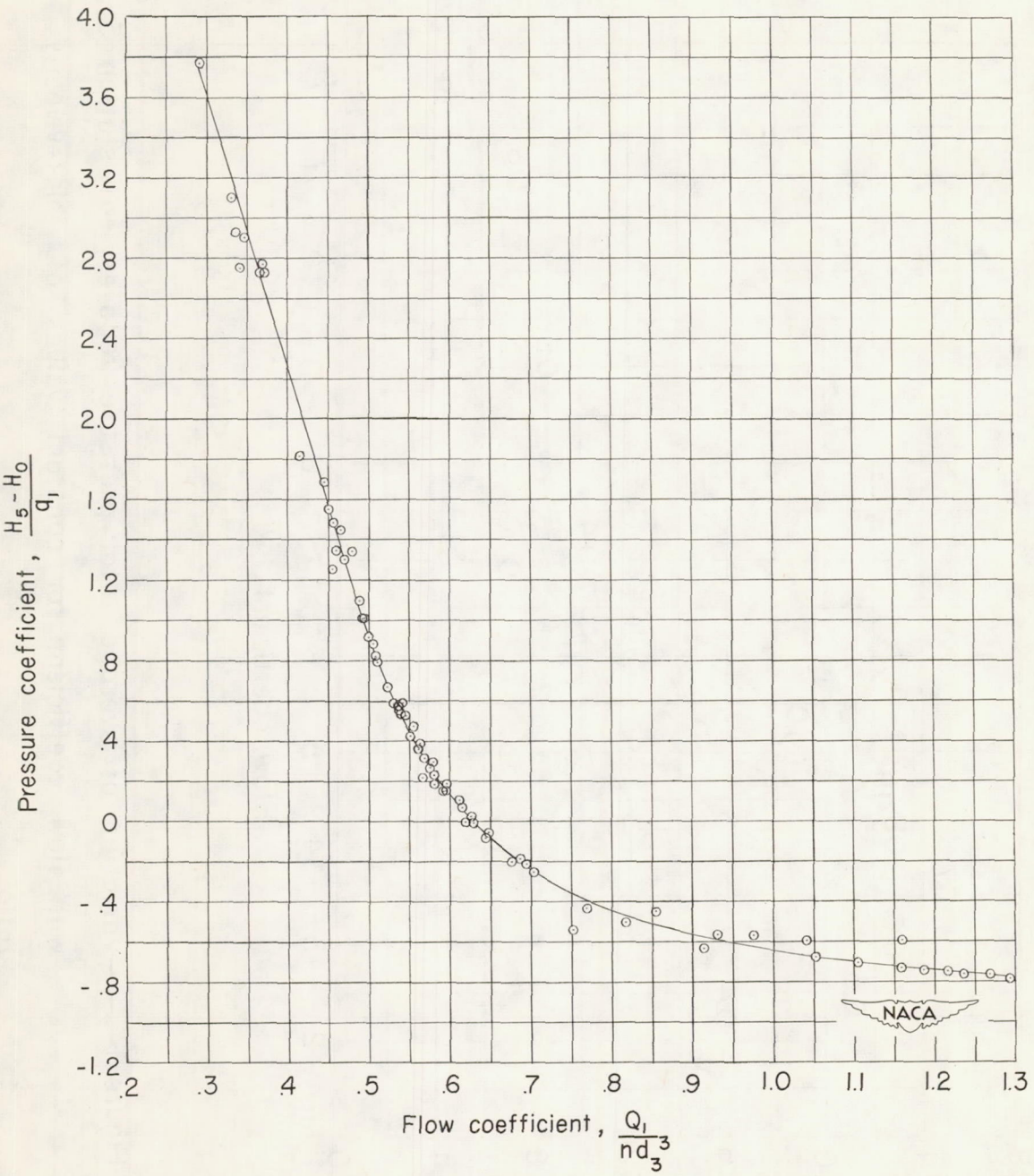

Figure 15.——Variation of average total-pressure coefficient at station 5 with flow coefficient.

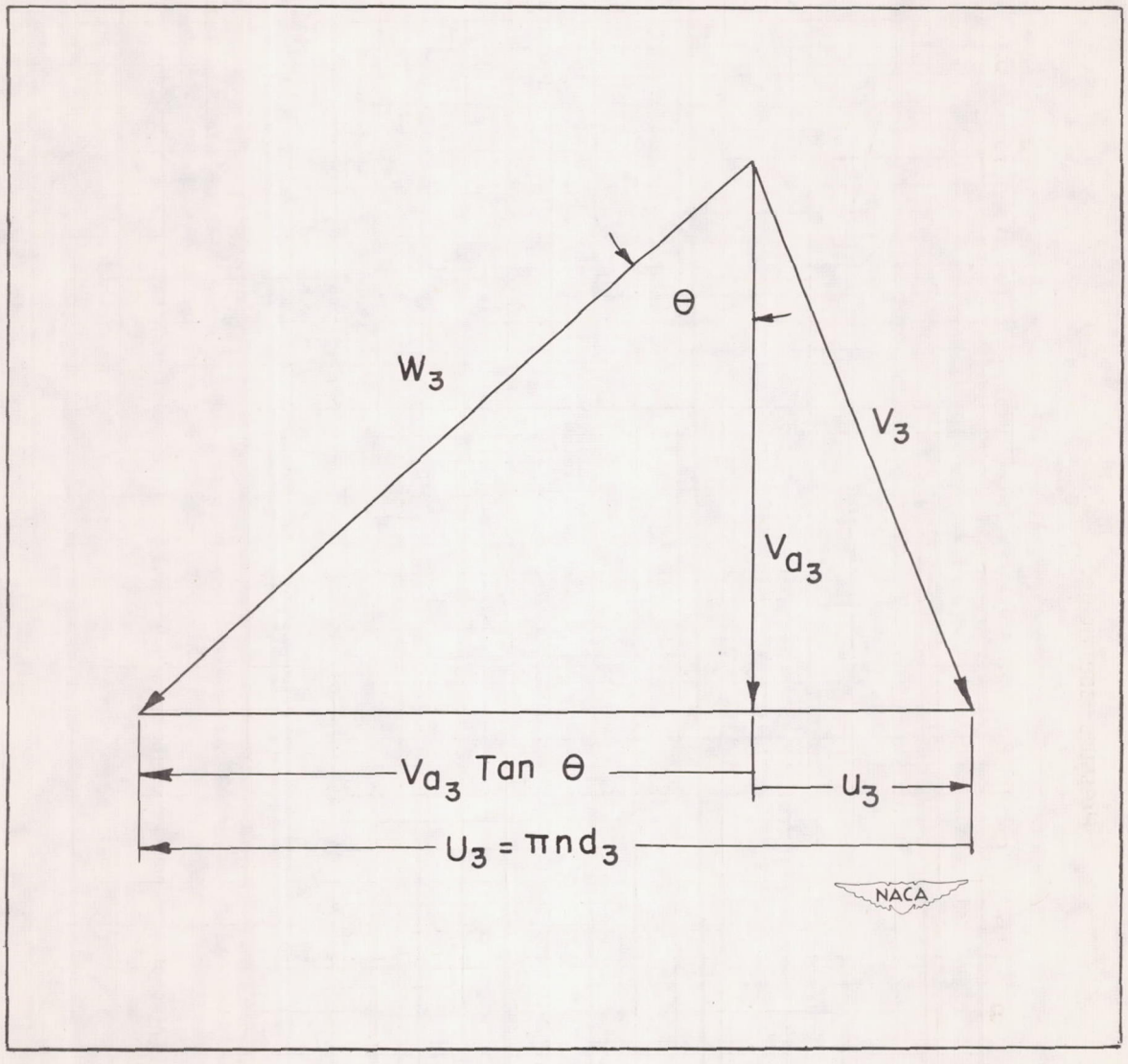

Figure 16. — Vector diagram at vane outlet. (station 3)

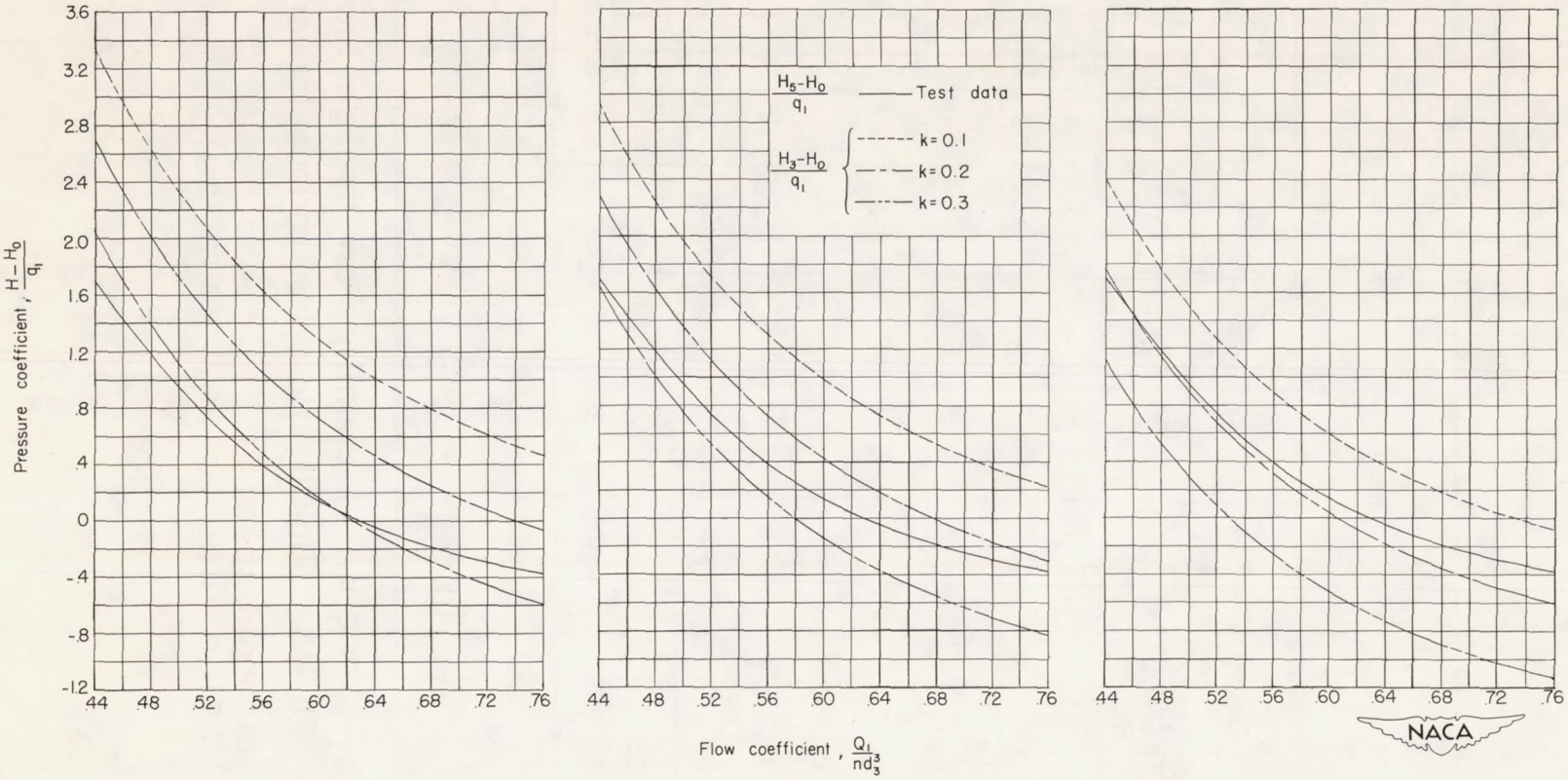

(a) $\theta = 50°$ (b) $\theta = 55°$ (c) $\theta = 60°$

Figure 17.— Comparison of the variation of pressure coefficient with flow coefficient calculated from equation (4) with test data.

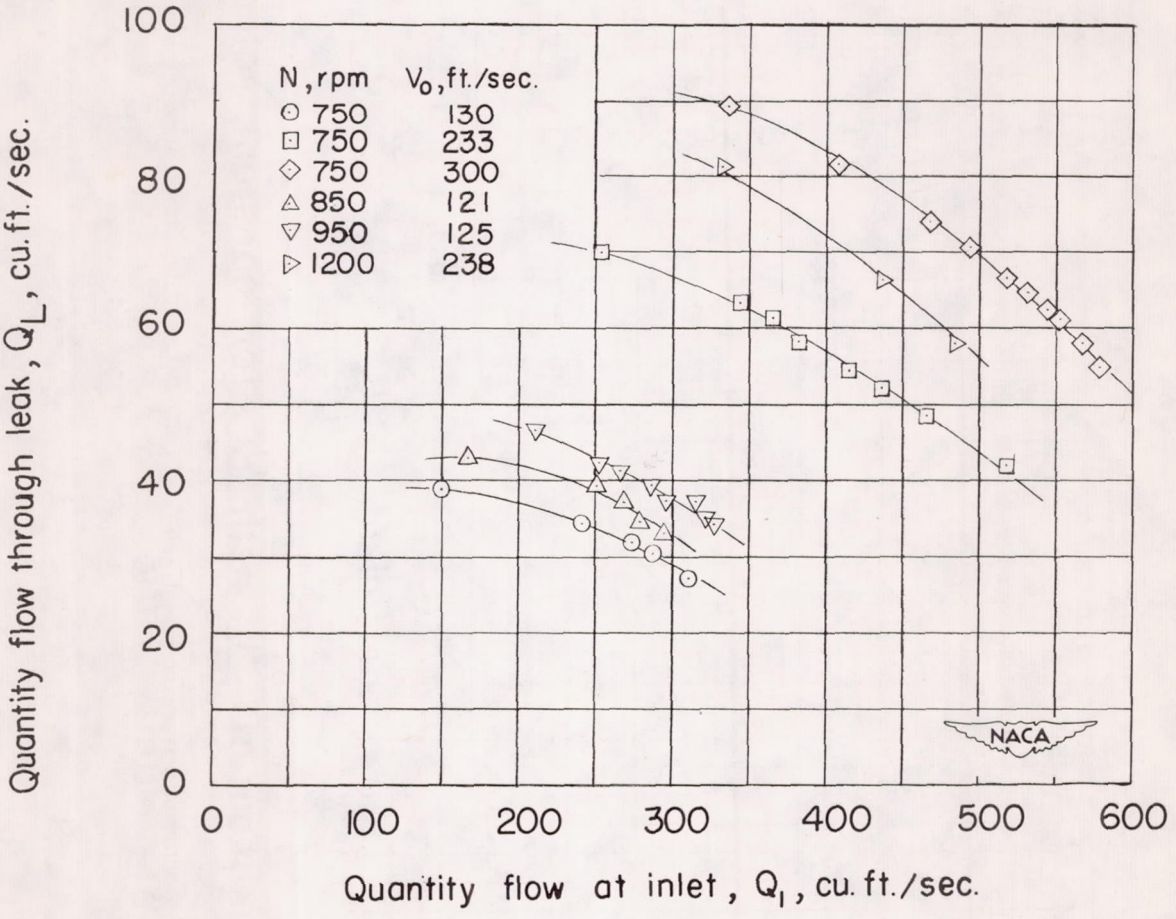

Figure 18.— Variation of quantity flow through leak gap with inlet quantity flow for various forward and rotational speeds.

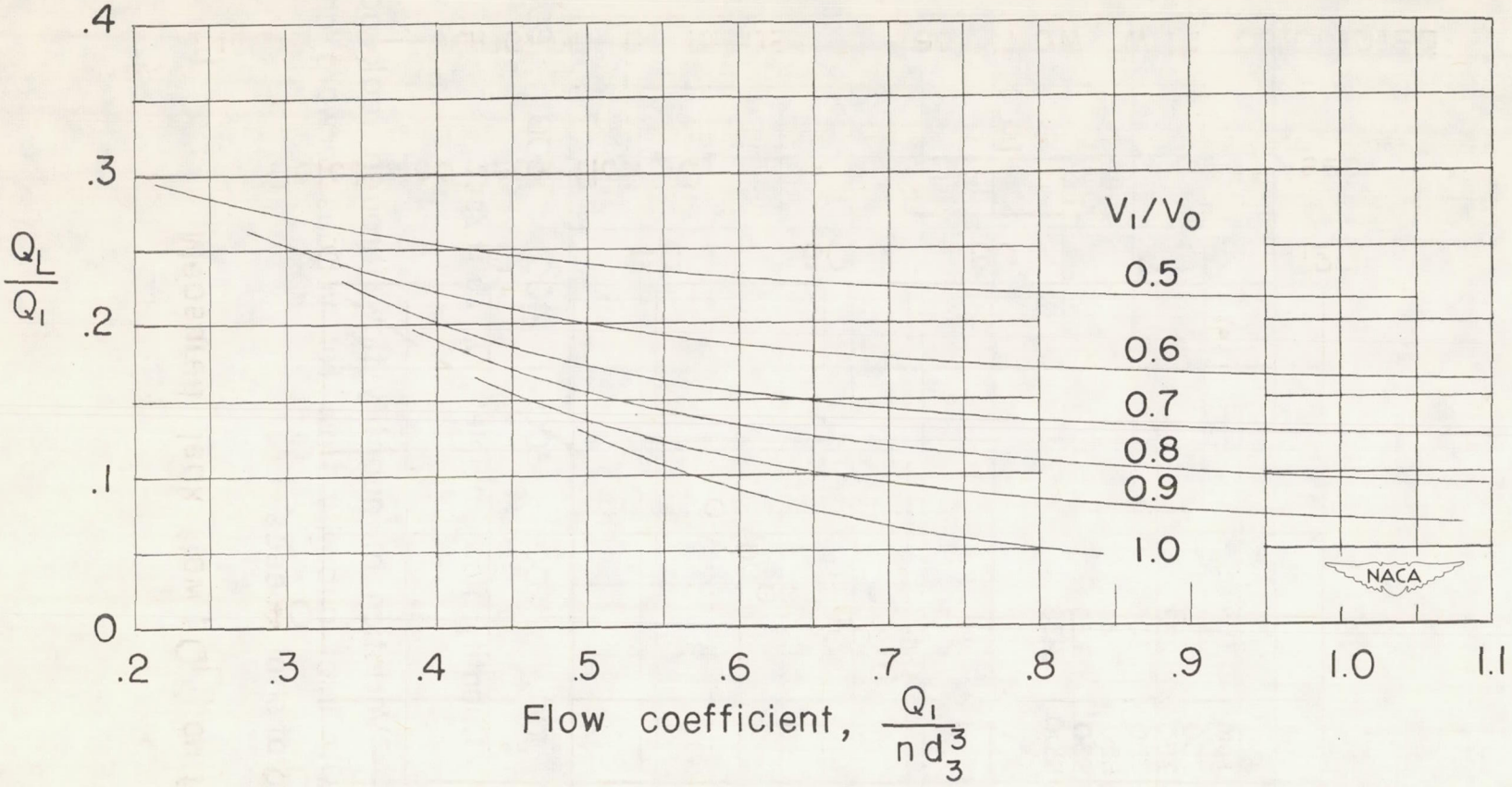

Figure 19. — Variation of $\frac{Q_L}{Q_1}$ with $\frac{Q_1}{nd_3^3}$ for constant values of inlet-velocity ratio.

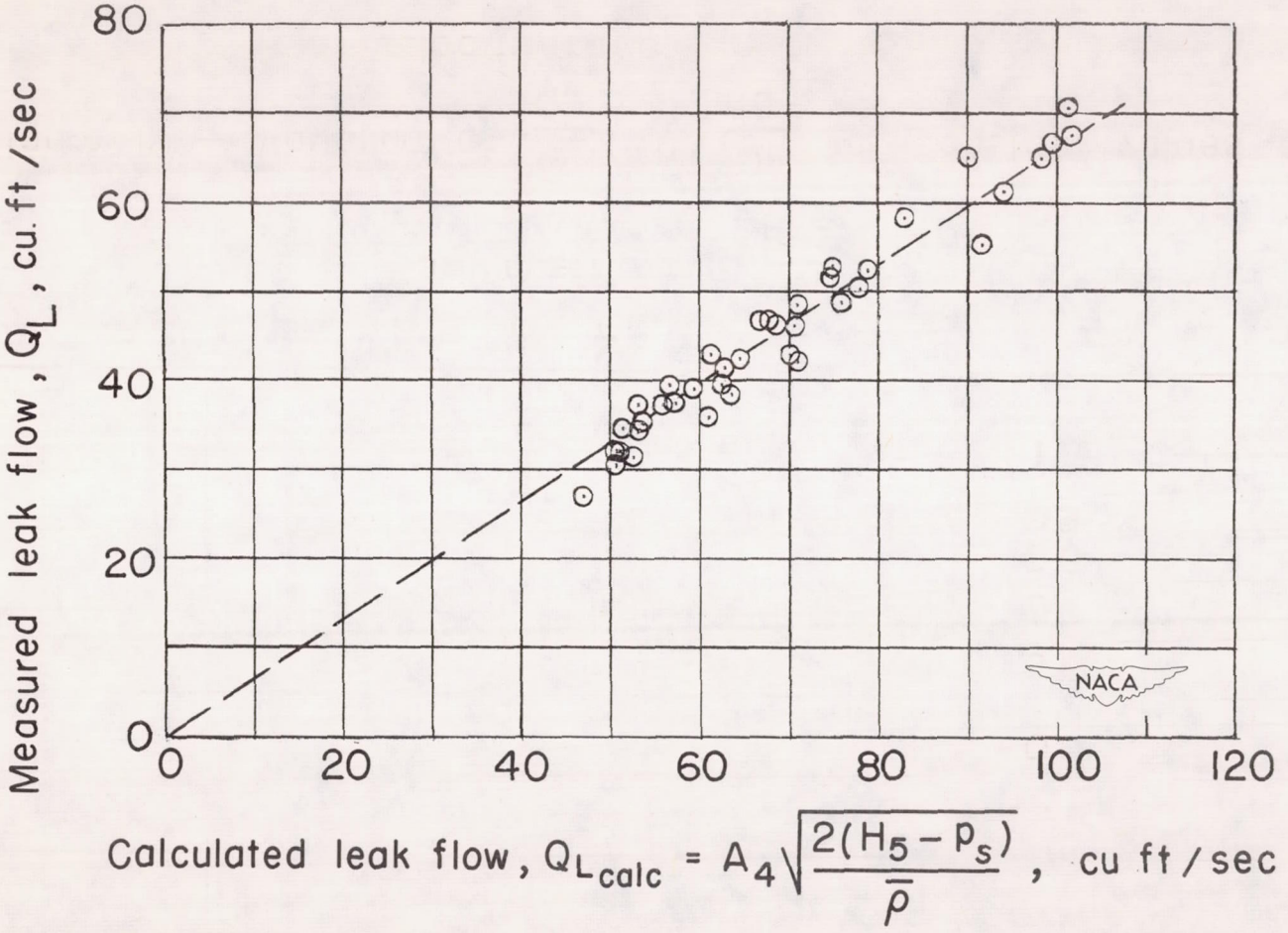

Figure 20.—Variation of measured leak flow with calculated leak flow.